Comparison of Doses to Normal Brain in Patients Treated With Boron Neutron Capture Therapy at Brookhaven National Laboratory and MIT

By

Julie Catherine Turcotte

B.S. Nuclear Engineering and Engineering Physics (2002)
Rensselaer Polytechnic Institute

Submitted to the Department of Nuclear Engineering
In Partial Fulfillment of the Requirements for the Degree of
Master of Science in Nuclear Engineering

At the

Massachusetts Institute of Technology

August 2004
[September 2004]

© 2004 Massachusetts Institute of Technology
All rights reserved

Signature of Author _____
Department of Nuclear Engineering
August 2004

Certified by _____
Jeffrey A. Coderre
Associate Professor of Nuclear Engineering
And Rasmussen Professor of Nuclear Engineering
Thesis Supervisor

Read by _____
Otto K. Harling
Professor of Nuclear Engineering
Thesis Reader

Accepted by _____
Jeffrey A. Coderre
Chairman, Department Committee on Graduate Students

ARCHIVES

MASSACHUSETTS INSTITUTE OF TECHNOLOGY
OCT 11 2005
LIBRARIES

Comparison of Doses to Normal Brain in Patients Treated With Boron Neutron Capture Therapy at Brookhaven National Laboratory and MIT

By

Julie Catherine Turcotte

Submitted to the Department of Nuclear Engineering
On July 31, 2004 in Partial Fulfillment of the
Requirements for the Degree of Master of Science in
Nuclear Engineering

ABSTRACT

A number of boron neutron capture therapy (BNCT) clinical trials are currently underway around the world. Due to the small number of patients at each of the individual centers, it is desirable to pool the clinical data from each into one patient database. Before this can be done, a number of differences between the clinical centers must be evaluated. The patients treated at the BNCT centers at Brookhaven National Laboratory and that at Harvard-MIT will be evaluated as a start to the ultimate pooling of all the BNCT centers. One difference involves the difference between the normal tissue composition definition between the institutions. In particular, the difference in weight percent of ^{14}N must be evaluated. This particular component of tissue is of importance due to the dose to tissue resulting from the $^{14}N(n,p)^{14}C$ reaction. The difference between the 1.8% ^{14}N composition used at BNL and the 2.2% used at MIT has a negligible effect on the total dose. Most importantly, differences in dosimetry techniques between the different centers must be computed. Once these differences are quantified, the patients can be pooled, and a better estimate of the normal brain tolerance to BNCT can be determined. The thermal neutron doses calculated from thermal flux measurements are 8% lower when measured by MIT, the gamma dose measurements are 26% lower, and the in-air fast neutron measurements are 27% lower in the same beam. The endpoint used for the tolerance of normal brain to BNCT is somnolence syndrome. A 50% somnolence response can be seen at 5.5 Gy-Eq.

Thesis Supervisor: Jeffrey A. Coderre
Title: Associate Professor of Nuclear Engineering and Rasmussen Professor of Nuclear Engineering

Acknowledgements

First, I would like to thank my advisor, Dr. Jeffrey Coderre. With his patience and guidance, I was able to conduct this research. Thanks also to Dr. Otto Harling who acted as my thesis reader. His advice and suggestions were integral to my success.

Many thanks must also be extended to Ray Albritton. His immense knowledge of the RTPE and SERA planning systems saved the day a number of times. The expertise of Chuck Wemple and Jacek Capala was also essential in running RTPE, and my thanks go out to them.

Thanks to Dr. Peter Binns and Dr. Kent Riley at the MIT research reactor, and to Dr. Stead Kiger at Beth Israel Deaconness Hospital in Boston for their input, experience, and expertise on the topic of BNCT. Thanks also to Dr. John Hopewell in Cambridge, England, for his help with the statistical dose response curves.

I would like to thank a few of my undergraduate professors at RPI, namely Drs. Yaron Danon, Don Steiner, Bimal Malaviya, and George Xu. Without their guidance in the first four years of my nuclear engineering education, I wouldn't be here today.

I would like to thank the other students in the lab here at MIT: Peter, Paige, Jingli, Brett, Mike, Ray, Yoonsun, Xuping, Rong, and Hongyu. Working with them has made being here much more enjoyable, and I'll miss you all when I leave here.

Lastly, I would like to thank my friends and family, without whose support I could never have done this.

Table of Contents

Tables

Figures

I. Background

1. BNCT

Boron neutron capture therapy (BNCT) is an experimental binary radiation treatment modality currently being tested against types of cancer that have proven difficult to treat by traditional means, such as the primary brain tumor glioblastoma multiforme (GBM). BNCT relies on the thermal neutron interaction with ^{10}B, which has a high thermal neutron capture cross-section. A tumor-selective boron-labeled compound is administered to the patient, followed by neutron irradiation. When the ^{10}B nucleus interacts with a thermal neutron, it emits an alpha particle and a ^{7}Li ion through the $^{10}B(n,\alpha)^{7}Li$ reaction. These emitted particles both have very short path lengths in tissue (about 9μm for the alpha particles and about 5μm for the ^{7}Li [1]); these distances are about the same as the diameter of a cell. Because of this, the damage caused by the energy deposition of the alpha particles will occur close to the location of the original ^{10}B interaction.

BNCT treatment of tumors is quite different than conventional radiotherapy treatment of tumors. The photon beams used for conventional radiotherapy are targeted to the tumor. They are sharply collimated, and can be shaped according to the best treatment plan. For instance, in gamma knife treatment, multiple pencil beams are used, and they all cross at the tumor, which allows for maximum dose to be administered to the tumor tissue, while sparing the normal tissue. Therefore, in conventional radiotherapy, normal tissue sparing comes from beam geometry and collimation. In BNCT, low-energy neutrons are needed for the neutron capture reaction in boron. These low-energy neutrons scatter once they enter tissue. Because of this, a dose is administered to the entire treatment region. Both the tumor and a considerable volume of surrounding normal tissue are exposed to neutrons, and there is always a non-specific background beam dose administered to the normal tissues. If capture compounds with good selectivity are used, then the dose to normal tissue is less than the dose to tumor tissue. Thus, in BNCT, normal tissue sparing comes from selective accumulation of boron in the tumor, and BNCT can be used to destroy tumor cells that microscopically infiltrate into normal tissues. BNCT should be thought of as a tumor-targeting therapy at the cellular

level. With suitable compounds and neutron beams, BNCT can, in principle, control cancer in large tissue volumes such as whole brain without unacceptable damage to normal brain. BNCT can also, in principle, kill individual tumor cells while sparing the adjacent normal cells. Average therapeutic ratios of about 3 to 4 can be calculated for BNCT using the currently available capture compound boronophenylalanine (BPA).

In clinical trials, BNCT has mainly been used to treat malignant gliomas, particularly glioblastoma multiforme (GBM). GBM accounts for about 80% of all malignant gliomas, and is one of the most intractable brain tumors. Despite conventional treatments (surgery, chemotherapy, traditional radiotherapy), patients with GBM have a median survival time of 9 to 10 months, and a 5-year survival rate of <5% [2]. GBM is a highly invasive tumor, with tumor cells infiltrating deeply into the surrounding brain tissue, creating microscopic islands of tumor cells set apart from the main tumor. These infiltrating tumor cells cannot be killed by conventional radiotherapy because a dose large enough to kill them would be administered to normal brain tissue as well, and such a high dose could cause brain damage. Because of this, BNCT is being investigated as an alternative means of treating these types of tumors. Given sufficient tumor-selectivity of the boron-containing compounds, BNCT would have the ability to treat these infiltrating tumor cells without causing significant damage to the surrounding normal brain tissue by allowing for a much lower total dose of radiation to be administered to the normal brain.

2. BNCT Clinical Trials

Table 1 lists the details of the major clinical trials of BNCT around the world [3]. The first clinical trial of BNCT for patients with GBM began in 1951 at Brookhaven National Laboratory (BNL), in the Brookhaven Graphite Research Reactor (BGRR). Over the next 8 years, three series of patients were irradiated there. The BGRR was originally built as a physics facility and therefore was not ideal for BNCT (it had no medical facility, no treatment room, no beam shutter, etc.). Results from clinical trials run at this facility were unsuccessful. The lack of success in these clinical trials was due mainly to problems with the boron compounds available at the time. These compounds did not exhibit tumor selectivity; they instead relied on the blood brain barrier to keep ^{10}B

out of the normal brain tissue. This led to high concentrations of ^{10}B in the blood, which resulted in damage to the brain and skin. In the mid 1950's the Brookhaven Medical Research Reactor (BMRR) was designed and constructed primarily for use in BNCT. The BMRR became operational in 1959. Over the following two years, a number of patients with brain tumors received BNCT at the BMRR [1]. During these trials, patients were given one of a number of boron-carrying compounds and irradiated with a thermal neutron beam.

At the same time (between 1959 and 1961), patients were also being treated with BNCT at the Massachusetts Institute of Technology reactor (MITR). During these trials, a number of different boron compounds and thermal neutrons were used in combination with a variety of surgical interventions. Results from both the BNL and MIT studies were disappointing and all clinical trials of BNCT in the United States were halted in 1961. The disappointing results arose from two primary causes. The first was that the thermal neutron beams did not penetrate very far into tissue. Because of this, there was inadequate thermal neutron fluence at depth (i.e., if the tumors were deep-seated enough), and some damage was also observed in the patients' skin. Secondly, low tumor to blood ratios were achieved with the boron-containing compounds available at the time. Both of these problems led to damage to the scalp and to the blood vessels in the brain.

The late Hiroshi Hatanaka began BNCT trials in Japan in 1968 at the Hitachi Training Reactor (HTR). Prior to this, Hatanaka had worked with Dr. William Sweet, who was pioneering much of the U.S. BNCT research, at Massachusetts General Hospital where he had learned surgical intraoperative procedures for BNCT. Over the course of the next 33 years (between August 1968 and July 2001), 183 patients with malignant brain tumors were treated with BNCT using a boron "cluster" compound $Na_2B_{12}H_{11}SH$, or BSH, and thermal neutron irradiation at 6 different reactors in Japan (however 10 patients since 1998 have been treated with epithermal neutrons under a new protocol). The tumor-to-blood boron concentration ratio was typically around 1.2-1.69 for BSH in these trials [4]. Results from these patients were more promising than those previously treated in the United States. Out of 105 patients, 29 with Grade 2, Grade 3, or Grade 4 gliomas survived for longer than 3 years [4].

BNCT reemerged in the United States after improvements were made in both boron compounds and neutrons beams in the late 1980s. At this point, higher-energy epithermal neutron beams (0.5 eV < E < 10 keV) were created at both the BMRR and the MITR. These higher energy neutrons are moderated as the beam penetrates into tissue to become low-energy thermal neutrons, which can then be captured by the boron-containing compound in tumor tissue. This allows for tumors that are found deeper in the brain to be treated with BNCT, and it decreases the risk of damage to skin, since the thermal neutron flux is low at the surface in contrast to the thermal neutron beams where the highest flux is at the skin.

In 1997, a Phase I trial for BNCT began in Petten, the Netherlands. Three years later, another trial began in the Czech Republic. These two studies treat brain tumors using the boron compound, sodium borocaptate [5]. Two other European trials, one in Finland and one in Sweden, have been treating GBM patients using the boron compound boronophenylalanine (BPA). All of the European studies have used epithermal neutron beams. A detailed review of all BNCT clinical trials is beyond scope of this thesis.

The most recent clinical trial at BNL ran from 1994 until 1999. During this time, 53 patients were treated with BNCT [2, 6]. Over the course of those 5 years, a number of changes in the treatment occurred. One change was simply prescribed by the definition of the clinical study. The clinical trial was a dose-escalating study, and therefore both the peak brain dose and the whole-brain average dose received by the patients was increased over time. Also, the treatment at BNL changed from a one-field treatment to a two-field treatment, and ultimately to a three-field treatment. Increasing the number of fields allowed for more uniform dose delivery to tumor and target volumes (target volume was defined as tumor volume plus a 2 cm margin around the tumor). Combining fields also allows for a higher peak in the target region, and lower doses to normal tissue. Additionally, a new collimator was created (the old collimator was 8 cm in diameter with a 13.1 cm thickness, and the new collimator was 12 cm in diameter with a 20.7 cm thickness), and the fuel rods in the reactor were rearranged in 1996. This caused desirable changes in neutron and photon flux intensities.

In 1994, epithermal neutron BNCT irradiation of peripheral metastatic melanoma were initiated at the MIT reactor (MITR), and this was followed by the brain tumor

clinical trial at Harvard-MIT begun in 1996 to evaluate normal tissue tolerance as well as tumor response. Between that time and May 1999, 22 patients were treated with BNCT using the MIT M67 beam. All of these patients were treated for either GBM or melanoma. As with the BNL trial, the number of fields used varied from one to three over the three years of the clinical trial, resulting in a progressive increase in both the peak dose and the whole-brain average dose. Harvard-MIT used the compound BPA, at doses of either 250mg/kg over the course of 1 hour, 300mg/kg over 1.5 hours, or 350mg/kg over 1.5-2 hours. The M67 epithermal neutron beam was used at MIT for the 22-patient phase-I trial, and it was equipped with a 15cm collimator [7]. This beam was located underneath the MITR, and the beam was directed downwards from the ceiling. Due to limitations in the M67 beam (such as low flux of epithermal neutrons and patient positioning difficulties), in 2001 a new fission converter beam (FCB) was constructed at MIT. This new beam has higher neutron intensity and less contamination from fast neutrons, slow neutrons, and photons [24]. Since this beam was built, 6 patients have been irradiated in a Phase I/II trial of BNCT with epithermal neutrons there. These patients are not included in this thesis because the data have not yet been published and the clinical records are unavailable at this time.

Table 1: Description of BNCT clinical trials around the world over the past 40 years [3]

Facility	# of Patients	^{10}B Compound	Infusion Time	Infusion Amount (mg/kg)	Ave. BBC[1] (μg ^{10}B/g)	Peak Brain Dose (Gy-Eq)	Ave. Brain Dose (Gy-Eq)
HTR, MuITR, JRR, KUR Japan	183 (1968–present)	BSH	1hr	100	~20-30	15 Gy[2]	NA
The Netherlands	26 (1997-present)	BSH	100 mg/kg/min	100	30[3]	8.6-11.4Gy[4] ^{10}B component	NA
LVR-15 Rez Czech Rep.	5 (2001-pres.)	BSH	1 hr	100	~20-30	< 14.2	< 2
BMRR Brookhaven, USA	53 (1994-1999)	BPA	2 hr	250-330	12-16	8.4-14.8	1.8-8.5
MITR-II, M67 MIT, USA	22[5] (1996-1999)	BPA	1-1.5 hr	250-350	10-12	8.7-16.4	3.0-7.4
MITR-II, FCB MIT, USA	6 (2001-pres.)	BPA	1.5 hr	350	~15	7.0-7.7	6.90-7.80
Studsvik Sweden	17 (30)[6] (2001-pres.)	BPA	6 hr	900	24 (range: 15-34)	7.3-15.5	3.3-6.1
Fir 1 Finland	18 (1999-pres.) protocol P-01	BPA	2 hr	290-400	12-15	8-13.5	3-6 <7
Fir 1 Finland	3 (2001-pres)[7] protocol P-03	BPA	2 hr	290	12-15	< 8	2-3 < 6

[1] BBC = blood boron concentration during the irradiation. [2] ^{10}B physical dose component dose to a point 2 cm deeper than the air-filled tumor cavity. [3] 4 fractions, each with a BSH infusion, 100 mg/kg the first day, enough to keep the average blood concentration at 30 mg ^{10}B/g during treatment on days 2-4. [4] ^{10}B physical dose component at the depth of the thermal neutron fluence maximum. [5] Includes 2 intracranial melanomas. [6] J. Capala, unpublished, personal communication with J. Coderre. [7] Retreatment protocol for recurrent glioblastoma.

3. Boron compounds and radiobiology

Over the years, a number of different compounds have been developed which show preferential accumulation in tumors, though only two of these have reached the stage of BNCT clinical trial: p-boronophenylalanine fructose (BPA-F, or simply BPA) and sulfhydryl borane (BSH). BPA was first synthesized in the late 1950s for BNCT, but was initially set aside due to the fact that it penetrates the blood-brain barrier, which at the time was seen as a significant disadvantage. BPA was later used for treatment of melanomas due to its structural similarity to melanin precursors [8]. In biodistribution studies, BPA was found to selectively accumulate in rat 9L gliosarcomas [9]. While the brain-to-blood boron concentration ratio was approximately 1, the tumor-to-blood/brain boron concentration ratios were found to be closer to 3:1 or 4:1 [13]. This is most likely due to elevated transport of amino acids at the tumor cell membranes [11]. Using ion microscopy, intracellular boron was found to be uniformly distributed across the cytoplasm and the nucleus in vitro and in implanted 9L brain tumors in rats injected with BPA. The boron concentration in tumor clusters infiltrating the normal brain was found to be about 50% of that in the main tumor for the BPA administration protocol that was used [12]. BPA-based BNCT produced long-term control of over 90% of rats having implanted 9L brain tumors [13].

As opposed to BPA, BSH does not cross the blood-brain barrier. It is able to accumulate in tumors due to the fact that blood vessels in intracranial tumors lack a properly functioning blood-brain barrier. Animal models showed a tumor to blood boron concentration ratio of about 0.5:1 to 1:1 [14], but this ratio has been found to be somewhat higher in human GBM patients. Hatanaka and Nakagawa have found a tumor-to-blood boron concentration ratio of about 2:1 at 17.5 hours after the end of the compound infusion in 39 patients, and four European centers showed ratios of about 1.3:1 to 2:1 [15].

Currently, BSH is mainly used in the Japanese trials, as well as a few of the European trials. BPA was the compound used during the BNL trials and was used at the Harvard-MIT trials, as well as in trials in Sweden. Patients treated with doses of 250 mg BPA/kg at BNL showed no signs of toxicity after a 2-hour infusion [16], and in fact levels up to

350mg BPA/kg have been administered to patients in the Harvard-MIT trials with a 1.5-hour infusion time [7]. In Sweden, doses up to 900mg/kg administered over 6 hours, resulting in average blood-boron concentrations of 24μg/g at the time of irradiation, have been administered to patients during a 6-hour infusion with no toxicity [17]. Both BPA and BSH are administered to the patient intravenously. Using subcellular secondary ion mass spectrometry (SIMS) on human glioblastoma cells incubated in vitro with ^{10}B-labeled BPA-F or ^{11}B-labeled BSH, or both, intracellular levels of ^{10}B from BPA-F were found to nearly double between 1 h and 6 h incubations, with a 3:1 intracellular to nutrient medium partitioning, while intracellular levels of BSH remained essentially unchanged in both single- and mixed-drug treatments [18].

The total radiation dose received by a BNCT patient is comprised of several different components; this is due in part to beam contaminants (photons), different neutron interactions that occur in tissue (protons from the $^{14}N(n,p)^{14}C$ reaction and photons from neutron capture in tissue hydrogen, the $^{1}H(n,\gamma)^{2}H$ reaction), and differences in the distribution patterns of the boron compounds, as described above. Therefore, the total dose is made up of a thermal neutron component, a fast neutron component, a gamma component, and a boron component. To sum all these together requires expressing each in a "photon-equivalent" unit to make it possible to compare against conventional photon irradiation. To do this, relative biological effectiveness (RBE) factors must be applied to each component. The RBE for each dose component has been determined experimentally [14]. Typically, the RBE of a given type of radiation is due only to the radiation's linear energy transfer (LET). In the case of the boron dose component in BNCT, this is not true; the biological effect of boron also depends on which compound is being used (i.e., specific microscopic distribution characteristics of the boron compound must be taken into account). Because of this, instead of RBE, the term compound biological effectiveness (CBE) factor is used. A "beam RBE" can be determined in the absence of boron-10 by comparing a neutron beam dose with an X-ray dose sufficient to produce an isoeffect. Once this beam RBE has been determined, the boron CBE can be determined. Additionally, the individual fast and thermal neutron RBE factors can be determined once the beam RBE has been determined. For each tissue and each boron compound, the RBE and CBE factors can be determined using appropriate normal tissue

irradiation models and comparing the x-ray dose, the neutron-only dose, and the neutron plus boron dose required to produce an isoeffect [14]. Once each of the RBE factors has been determined, they can be multiplied by their corresponding dose components and summed together to obtain a total weighted dose, in units of gray-equivalent (Gy-Eq).

4. BNCT Treatment Planning

There are two primary treatment planning software programs available for BNCT. Since this thesis focuses mainly on combining clinical data from the BNL and Harvard-MIT programs and the differences in dosimetry and treatment plans between these centers, discussion of treatment planning software will be limited to those used at these two facilities: namely, Radiation Treatment Planning Environment (RTPE), as well as some mention of its successor, Simulation Environment for Radiotherapy Applications (SERA), both of which were used at BNL, and MacNCTPlan/NCTPlan, which is used at MIT. RTPE and SERA were developed by a collaboration of the Idaho National Engineering Laboratory (INEL) and the computer science department at Montana State University [19], and were used by the BNCT group at BNL. The BNCT group in Sweden is also currently using SERA. MacNCTPlan and NCTPlan were developed and used by the BNCT group at MIT. These programs all rely on Monte Carlo codes to transport particles through tissue. However, beyond this basic similarity, there are a number of other differences in the software programs, and these differences may give rise to differences in patient treatment plans. Therefore a description of the main characteristics of each program is necessary for a complete comparison of clinical trials at different institutions.

Before BNCT treatment planning software was developed, scientists determined that a Monte Carlo (MC) code would be the most useful tool to use in creating a patient treatment plan. In conventional MC codes, it is difficult to obtain the necessary detailed edits for BNCT. While volume-integrated results are typically obtained automatically with most MC codes, special edits must be performed to obtain the necessary output for BNCT, such as dose volume histograms and isodose contours. Additionally, the patient geometry would need to be modeled by hand for use in MCNP, instead of being able to

utilize CT or MRI scans. This would result in a significant increase in total treatment planning time, due to the time it would take to create the special edits and then the extra time it would take to run enough particles for statistical significance. This led to the development of BNCT_edit, which is based on a Monte Carlo code called Raffle. Raffle was developed at the Idaho National Engineering Laboratory (INEL) in the 1970's, and in the 1980's it was extended to incorporate the most recent Evaluated Neutron Data File (ENDF-V), resulting in Raffle V. By the 1990's, BNCT_edit was replaced with BNCT_rtpe, which was first used in the BNL BNCT clinical trials in 1994 [19]. This program is more commonly referred to as Radiation Treatment Planning Environment, or RTPE. Contained in this program is the particle transport code called radiation transport in tissue by Monte Carlo (better known as rtt_MC), which is the part of RTPE that runs particles through a specified geometry and makes tallies of information that is of particular interest to the user.

In rtt_MC, the true patient geometry is used rather than an approximation in order to obtain the detailed edits necessary for BNCT. CT or MRI images taken of the patient are loaded directly into RTPE, and a three-dimensional mesh is imposed over the top of these images. This "subelement mesh" does not affect particle transport or tracking, being that it is virtual and does not actually exist anywhere on the patient. As the particles are tracked through this mesh, tallies are performed to determine total dose, boron dose, gamma dose, nitrogen dose, fast neutron dose, neutron fluence for a specified number of energy bins, and induced gamma production [19].

RTPE makes use of non-uniform rational b-splines, or NURBS. NURBS provide a free-form curve and surface representation system, which incorporate the properties of b-splines, interpolating splines, and Bezier curves and surfaces [19]. The NURBS replaced a polygonal representation, in which simple geometric figures (such as cubes, cones, and cylinders) are used to model certain bodies. NURBS can model more complex shapes than polygonal geometry, and can more accurately depict the bodies on a CT or MRI scan. The "non-uniform" aspect refers to a knot vector. This knot vector is actually a series of nondecreasing scalar values that direct the curve about the control points [19]. In the RTPE environment, the user enters a number of control points to outline the surface of the different regions of interest on the individual MRI or CT scans, such as

skull, brain, and tumor. From these control points, the knot vector allows for continuity in the curves. The b-spline uses a weighting scheme to determine the contribution each control point makes to the position vector. At this point, RTPE then generates a file that is a NURBS representation of a three-dimensional model based on the MRI or CT images provided from the patient.

During the next few years of use, changes were made to the RTPE program to fix problems that arose with the program during the clinical trials. Ultimately, an entirely new program known as the Simulation Environment for Radiotherapy Applications (SERA) was created. While both programs were created with the same basic structure, SERA is different from RTPE in a few important ways. First, SERA is based on a pixel-by-pixel uniform volume element (known as a "univel") reconstruction. Different bodies are identified on the computer by filling in the pixels associated with each with a different color. A name is given to each of these bodies, and information about each of these bodies is available in the program: information such as elemental composition, RBE factors of the various dose components, etc. The use of these univels gives SERA the advantage of much shorter execution time for the transport calculations than RTPE.

Beam alignment in RTPE is done in the input file. The user specifies the beam alignment by entering on the required line of the input file the beam's distance from a point in the patient's head, the rotation about the azimuthal angle, as well as the rotation about the polar angle. While the user-specified target point on the patient's head remains fixed, the neutron source is rotated about this point. Both RTPE and SERA allow for different types of output from the patient treatment plan. For instance, the user can choose to output a dose-volume histogram (either for the whole brain, a particular hemisphere, the tumor, etc.). Additionally, the user can output an isodose contour, which will allow the user to determine if the chosen plan is administering too high a dose to a particular region of the patient's brain.

The program used in the Harvard-MIT clinical trials is called NCTPlan. It was initially designed around 1990, and was created to optimize the existing beam design (dimensions, orientation, energy). The brain model used in this program is called Neutron Photon Brain Equivalent (NPBE) model, and is created by two non-concentric

ellipsoids. The elemental composition of this model has been documented by Zamenhof et al. [20].

In 1996, after computational improvements were implemented, a new version of NCTPlan was developed. This new version was written in Pascal, and called MacNCTPlan because it was developed for a Macintosh platform. This MacNCTPlan contains two major parts. Part I is where the three-dimensional mathematical model of the patient's head is created from a set of MRI or CT scans using a "voxel" technique. Part II is where the graphical environment exists, allowing the development of dose patterns from the results of the particle transport calculations. It is here that the dose distribution results can then be displayed in a one- two- or three-dimensional format.

Part I involves reconstructing the patient's head into a geometry form that the computer can use. To do this requires the use of "voxels". Voxels are cubes of volume 1 cm^3 (or possibly smaller), which are stacked in a three-dimensional array. A material is assigned to each voxel, and the definitions of these materials can be found in a separate material file. In MacNCTPlan, two sets of CT images are used: one with and one without an iodinated contrast agent. The images with no contrast are used to determine what type of tissue will make up the three-dimensional model for the MC calculations. The contrast-enhanced images are used to identify the tumor and other bodies within the head. This step is necessary to determine the region of interest (ROI), which contains the tumor. From the chosen ROI, a diagram of pixel number versus Hounsfield number (H), which is the measure of the X-ray absorbency, or density, of tissue, can be constructed. This diagram will yield three peaks: one for the soft tissue (cancerous or normal), one for the skull and one for the air. Each pixel is given a material assignment depending on its corresponding H value. The final model contains 11,025 calculation cells, each containing between 500-1000 voxels. A material is assigned to each cell by averaging between four basic materials (air, tumor, normal soft tissue, and bone), with a weighing factor depending on the number of voxels in a particular cell corresponding to each material [20].

An important step in any treatment plan is setting up the beam alignment. In MacNCTPlan, this means identifying the entrance and exit points of the beam's central axis on the patient. Up to four different beams can be used for treatment. Two

orthogonal viewing planes can be used through CT image data in MacNCTPlan. This allows for real-time updating when changes are made to the beam orientation, and thus the interaction of the beam with the patient's head model can be seen immediately. Also, the locations of the beam entrance and exit points are necessary for patient positioning during treatment. In MacNCTPlan, the neutron source is a plane source in a fixed position with regards to the three-dimensional head model. When the user changes the beam orientation, the software changes the location of the source plane, while the head model remains the same. Once the model is created, a Fortran 77 program, called MPREP, provides the MCNP input deck from a series of files. These files contain all the information required for computing the doses within the model, including angular and energy characteristics of the neutron and photon beams, material definitions, and values for the kinetic energy released in matter (KERMA).

Part II of MacNCTPlan allows for viewing the dose patterns extracted from the transport calculations that are performed by MCNP. These results (such as RBE isodose contours) can then be displayed in one- two- or three-dimensional format. Dose-volume histograms (DVHs) for the tumor, target volume, and whole brain can be generated as well. This gives the user information on dose distribution, and the percent of particular volumes subjected to a certain dose or dose rate. If multiple beams are to be used during treatment, MacNCTPlan combines them in the treatment plan according to their weight, which is generally defined as a function of the irradiation time.

A few years after MacNCTPlan was created, a new PC-based version of MacNCTPlan, again named NCTPlan, was created in collaboration with the Comision Nacional de Energia Atomica in Argentina (CNEA), Harvard Medical School, and MIT. It was written in Microsoft Visual Basic™ 6.0 and runs under Windows 95/98/NT and 2000 [21]. This code was developed in order to update certain parts of MacNCTPlan, as well as to create a software program that can be used on a more common computing platform. MPREP was integrated into this program, and NCTPlan can superimpose isodose contours on multiple orthogonal planes of the CT or MRI images. Another difference between MacNCTPlan and NCTPlan is in the material assignment model. Each image slice is constructed of a number of cells, and each of these cells is defined based on its mixture of air, soft tissue, tumor, and bone. The percent composition of each

of these materials is rounded off to the nearest percentage, but occasionally, the procedure of rounding does not yield a total percentage of 100% in each cell. When this happens, MacNCTPlan assigns to the cell the last admissible mixture calculated. NCTPlan on the other hand searches for the mixture that minimizes the sum of the relative differences (in absolute values). If this minimum value is not unique, the code chooses the arrangement that has the least effect on the particle transport [21]. Additionally, changes in the calculation of DVHs were performed, which reduce the errors due to the interpolation method.

As can be seen, RTPE and NCTPlan differ in a number of ways. Geometry reconstruction, material definition, and kerma coefficients are among the significant differences in the two programs. This thesis will not go into the effects of these differences on the patient treatment plans, but they should be considered for a complete pooling of patient data.

5. BNCT Intercomparison

Because of the small number of patients treated with BNCT, it is desirable to pool patient data from different BNCT facilities. As is clear from the above discussion, it is quite difficult to compare a patient treatment plan at one institution to one at a different institution. Therefore, before a complete pooling of patient data can take place, each of these differences must be evaluated. In particular, this thesis will focus on the differences between the clinical trials at MIT and BNL. Among these differences are material definitions (particularly elemental composition of ^{14}N in normal brain tissue), measurement of thermal neutron flux, fast neutron dose, and gamma dose at each institution, and geometry definitions.

Over the years, there has been no single common source of elemental compositions of tissue for all the institutions to use, and therefore different institutions use a different value for the weight percent of ^{14}N found in normal brain tissue. While BNL used a ^{14}N weight percent of 1.8 (the recommended value from an MIT workshop in 1989 [23]), Petten and Harvard-MIT have most recently been using a value of 2.2% (MIT originally used a value of 1.8%, however then switched in the past few years to use 2.2%), which is

the value recommended by the ICRU report 46 (see Table 2) [22]. The ^{14}N composition is particularly important because of the thermal neutron interaction that takes place with ^{14}N. Because of this difference in assumed ^{14}N concentration, the two institutions are actually stating that different ^{14}N doses will be administered to a patient. If these doses are significantly different, the effects may be seen in the total prescribed dose to the patients.

Another difference is the definition and measurement of thermal neutron flux, as well as fast and gamma dose measurement from one institution to another. Each institution measures its beam dosimetry in the way that they feel is most accurate. However, this means that most institutions are using different kinds of detectors, measuring in different phantoms, measuring at different depths down the center line of the beam axis, etc. For instance, at BNL, thermoluminescent dosimeters (TLDs) were used to measure the photon dose rate, while at MIT, ion chambers were used. This has caused a systematic difference in the doses reported by these different institutions for their respective beam components. TLDs are small and produce a minimum perturbation of the neutron field, but also are somewhat sensitive to thermal neutrons. This creates a high background that must be subtracted. Each type of detector has its own advantages and disadvantages, as well as each having its own associated error in a particular application. Because of this, even in the same beam, the two types of detectors could give different readings. When looking at a dose calculated from these measured values (such as thermal neutron dose calculated from thermal neutron flux measurements), the error will propagate, which causes concern when attempting to compare exposure from beams at different institutions. The error associated with the neutron beam measurements must be evaluated to determine the error associated with the prescribed dose. These measuring differences make an intercomparison of patient doses from the two different trials even more difficult.

Patient geometry at MIT and BNL is reconstructed using MRI or CT scans. When phantoms such as the Lucite cube are run in RTPE, a simple combinatorial geometry reconstruction is typically used. This is because phantoms such as the cube are more easily modeled using a geometric reconstruction, and CT scans are unnecessary. However, it is necessary to determine what effect the type of geometry (combinatorial vs.

NURBS) has on the peak and whole brain average doses. Differences in patient geometry within a single treatment planning system will be addressed later in this thesis.

As is quite obvious, the characteristics of the beams at different institutions are quite different from one another. When a neutron beam is extracted from a reactor, contaminating photons inevitably become part of the neutron beam. The extent to which these contaminants are a part of the beam is different from one facility to another. Each beam component must be thoroughly analyzed at each institution, and a direct means of comparing each component from one institution to another must be determined. This boils down to calculating a scaling factor for each dose component, allowing for a comparison of prescribed peak dose between two institutions.

The use of different treatment planning software programs can also cause problems when trying to compare patient data. For instance, NCTPlan and RTPE create the model geometry in very different ways. So, while both model the same patient's head, neither has created the head exactly, and the error associated with each modeling technique will lead to slight differences in the ultimate treatment plans. Additionally, no two codes are written exactly the same, and therefore differences in the particle transport and dose calculations may arise.

Since ultimately, a full pooling of BNCT patient data is desired, all of the differences between the participating facilities must be analyzed and evaluated. The effect of different ^{14}N concentrations, as well as scaling factors between the beam components must be determined. Once these differences are understood, the MIT and BNL patient data can be combined. The only normal brain side-effect observed in BNCT patients suitable for use in a combined data set has been somnolence, and when the MIT and BNL patients are combined, a more complete evaluation of the cause of this endpoint can be examined.

The objective of these Phase-I clinical trials at BNL and H-MIT is to determine safety and an estimate of normal tissue tolerance. The side effect observed in the central nervous system (CNS) of some of these patients was a somnolence syndrome. The objective of this thesis is to combine the clinical data from the BNL and MIT trials to create a stronger set of data for evaluation of the BNCT dose-response relationship in normal brain: in other words, an estimate of the tolerance of the normal brain to the

complex radiation field produced in tissue during BCNT. Such information on brain tolerance to BNCT will be of great importance in planning future clinical trials at MIT, as well as at all other clinical BNCT sites worldwide.

References:

1. D.N. Slatkin, A history of boron neutron capture therapy of brain tumours - postulation of a brain radiation dose tolerance limit, Brain, **114:** 1609-1629 (1991).

2. A.D. Chanana, J. Capala, M. Chadha, J.A. Coderre, A.Z. Diaz, E. Elowitz, J. Iwai, D.D. Joel, H.B. Liu, R. Ma, N. Pendzick, N.S. Peress, M.S. Shady, D.N. Slatkin, G.W. Tyson, L. Wielopolski, Boron Neutron Capture Therapy for Glioblastoma Multiforme: Interim Results from the Phase I/II Dose-Escalation Studies, Neurosurgery, **44:** 1182-1193 (1999).

3. J.A. Coderre, J.C. Turcotte, K.J. Riley, P.J. Binns, O.K. Harling, W.S. Kiger; Boron Neutron Capture Therapy: Cellular Targeting of High Linear Energy Transfer Radiation, Technology in Cancer Research & Therapy, **2:** 355-375 (2003).

4. Y. Nakagawa, K. Pooh, T. Kageji, S. Uyama, A. Matsumura, H. Kumada, Clinical Review of the Japanese Experience With Boron Neutron Capture Therapy and a Proposed Strategy Using Epithermal Neutron Beams, Journal of Neuro-Oncology, **62:** 87-99 (2003).

5. J. Burian, M. Marek, J. Rataj, S. Flibor, J. Rejchrt, L. Viererbl, F. Sus, H. Honova, L. Petruzelka, K. Prokes, F. Tovarys, V. Dbaly, V. Benes, P. Kozler, J. Honzatko, I. Tomandl, V. Mares, J. Marek, M. Syrucek, Report on the first patient group of the Phase I BNCT Trial and the LVR-15 Reactor, Essen, pp. 27-32 (2002).

6. A.Z. Diaz, Assessment of the results from the phase I/II boron neutron capture therapy trials at the Brookhaven National Laboratory from a clinician's point of view, J. Neuro-Oncol. **62:** 101-109 (2003).

7. P.M. Busse, O.K. Harling, M.R. Palmer, W.S. Kiger III, J. Kaplan, I. Kaplan, C.F. Chuang, J.T. Goorley, K.J. Riley, T.H. Newton, G.A. Santa Cruz, X-Q Lu, R.G. Zamanhof, A Critical Examination of the Results From the Harvard-MIT NCT Program Phase I Clinical Trial of Neutron Capture Therapy For Intracranial Disease, Journal of Neuro-Oncology, **62:** 111-121 (2003).

8. Y. Mishima, C. Honda, M. Ichihashi, H. Obara, J. Hiratsuka, H. Fukuda, H. Karashima, K. T., K. Kand, K. Yoshino, Treatment of malignant melanoma by single thermal neutron capture therapy with melanoma-seeking 10B-compound, Lancet, **2:** 388-389 (1989).

9. JA Coderre, JD Glass, RG Fairchild, PL Micca, I Fand and DD Joel, Selective delivery of boron by the melanin precursor analogue p-boronophenylalanine to tumors other than melanoma, Cancer Research, **50:** 138-141 (1990).

10. J.A. Coderre, E.H. Elowitz, M. Chadha, R. Bergland, J. Capala, D. D. Joel, H.B. Liu, D.N. Slatkin, A.D. Chanana, Boron neutron capture therapy for glioblastoma multiforme

using p-boronophenylalanine and epithermal neutrons: trial design and early clinical results, J. Neuro-Oncol. **33:** 141-152 (1997).

11. A. Wittig, W.A. Sauerwein, J.A. Coderre, Mechanisms of transport of p-borono-phenylalanine through the cell membrane *in vitro*, Radiat. Res., **153:** 173-180 (2000).

12. D.R. Smith, S. Chandra, J.A. Coderre, G.H. Morrison, Ion microscopy imaging of ^{10}B from p-boronophenylalanine in a brain tumor model for boron neutron capture therapy, Cancer Res., **56:** 4302-4306 (1996).

13. J.A. Coderre, T.M. Button, P.L. Micca, C.D. Fisher, M.M. Nawrocky, H.B. Liu, Neutron capture therapy of the 9L rat gliosarcoma using the p-boronophenylalanine-fructose complex, Int. J. Radiation Oncology Biol. Phys., **30:** 643-652 (1994).

14. J.A. Coderre, G.M. Morris, The Radiation Biology of Boron Neutron Capture Therapy, Radiation Research, **151:** 1-18 (1999).

15. H. Hatanaka, Y. Nakagawa, Clinical results of long-surviving brain tumor patients who underwent boron neutron capture therapy, Int. J. Radiat. Oncol. Biol. Phys. **28:** 1061-1066 (1994).

16. A.D. Chanana, M.D., Boron Neutron-Capture Therapy of Glioblastoma Multiforme at the Brookhaven Medical Research Reactor: A Phase I/II Study, Brookhaven National Laboratory, Upton, NY, January 2, 1996

17. J. Capala, B. H.-Stenstam, K. Skold, P.M. af Rosenschold, V. Giusti, C. Persson, E. Wallin, A. Brun, L. Franzen, J. Carlsson, L. Salford, C. Ceberg, B. Persson, L. Pellettieri, R. Henriksson Boron neutron capture therapy for glioblastoma multiforme: clinical studies in Sweden, Journal of Neuro-Oncology, **62:** 135-144 (2003).

18. S. Chandra, D.R. Lorey II, D.R. Smith, Quantitative Subcellular Secondary Ion Mass Spectrometry (SIMS) Imaging of Boron-10 and Boron-11 Isotopes in the Same Cell Delivered by Two Combined BNCT Drugs: *In Vitro* Studies on Human Glioblastoma T98G Cells, Radiation Research, **157:** 700-710 (2002).

19. D.W. Nigg, F.J. Wheeler, D.E. Wessol, J. Capala, M. Chadha, Computational dosimetry and treatment planning for boron neutron capture therapy, J. Neuro-Oncol. **33:** 93-103 (1997).

20. R. Zamenhof, E. Redmond II, G. Solares, D. Katz, K. Riley, S. Kiger, O. Harling. Monte Carlo-based treatment planning for boron neutron capture therapy using custom designed models automatically generated from CT data, Int. J. Radiation Oncology Biol. Phys, **35**: 383-397 (1996).

21. S.J. Gonzalez, G.A. Santa Cruz, W.S. Kiger III, J.T. Goorley, M.R. Palmer, P.M. Busse, R.G. Zamenhof. NCTPlan, the new PC version of MacNCTPlan: improvements

and verification of a BNCT treatment planning system, In: Research and Development in Neutron Capture Therapy, (eds W. Sauerwein R. Moss, A. Wittig), Monduzzi Editore, Bologna, Italy, 2002, pp. 557-561.

22. ICRU 46: Photon, electron, proton and neutron interaction data for body tissues, 1992

23. O.K. Harling, J.A. Bernard, R.G. Zamenhof (eds.), Proceedings of an International Workshop on Neutron Beam Design, Development, and Performance for Neutron Capture Therapy, Massachusetts Institute of Technology, Cambridge, MA (March 29-31, 1989).

24. K.J. Riley, P.J. Binns, O.K. Harling, Performance characteristics of the MIT fission converter based epithermal neutron beam, Physics in Medicine and Biology, **48:** 943-958 (2003).

25. W.S. Kiger III, X.Q. Liu, O.K. Harling, K.J. Riley, J. Kaplan, H. Patel, R.G. Zamenhof, Y. Shibata, I.D. Kaplan, P.M. Busse, M.R. Palmer, Preliminary treatment planning and dosimetry for a clinical trial of neutron capture therapy using a fission converter epithermal neutron beam, in press.

II. Materials and Methods

In comparing patient brain doses between clinical trials at two different clinical centers, it is necessary to quantify any differences in dose measurements based on systematic differences between different dosimetry techniques. Since the intercomparison of the patient doses in this thesis is based upon the dosimetry intercomparison reported by Riley et al. [1], a discussion of dosimetry techniques at BNL and MIT is warranted. MIT and BNL used different phantoms to perform routine dosimetry checks on their own beams, and also used different techniques to perform these measurements. To directly compare the dosimetry techniques, measurements were performed in the BNL beam by the MIT group in 1997 and 2000 using the standard BNL phantom, as well as the standard MIT phantom [1] and the results were compared to the published data from the BNL group [2]. The paper by Riley et al. [1] provides the basic data required for the brain dose comparison in this thesis. Since all factors were the same in both cases except for measurement techniques, a scaling factor between the MIT measured doses and the RTPE output can be obtained for each dose component. These scaling factors are a direct measure of the systematic differences in techniques. Again, since this thesis mainly focuses on the differences between clinical trials at MIT and BNL, only the dosimetry methods performed by each of these institutions will be detailed. Both the BNL and MIT phantoms can be run in the RTPE treatment planning system to benchmark the treatment plan against known measurements and to provide preliminary insight as to differences between the two treatment planning systems.

1. Dosimetry Phantoms

Routine dosimetry measurements were performed by MIT in their own beam using the MIT ellipsoidal water-filled phantom [3]. The ellipsoidal head phantom dimensions are 13.6 cm in the x-direction, 19.6 cm in the y-direction, and 16.6 cm in the z-direction, with a total volume of 2502 cm^3. The top two-thirds of the shell are made of acrylic, and the bottom third is made of acrylic plates. The definition of these materials can be found in Table 2. The shell is filled with distilled water, and watertight butyrate tubes are

inserted from the bottom of the phantom. This allows gold foils or ionization chambers that can be driven remotely by a computer-controlled stepper motor to be positioned within the water medium. During the gold foil irradiations the tube containing the foils is filled with water. When measurements are taken, the phantom is aligned with the beam on the patient treatment table along the phantom's x-axis. It is positioned so that there is no gap between the phantom and the plane of the end of the collimator. Figure 1 shows the Deutsch and Murray model of the head. This was used as the basis for the MIT head phantom. Figure 2 shows the dimensions and details of this phantom.

Table 2: Elemental composition for materials in the MIT ellipsoidal head phantom

Normalized Atomic Fractions

Material	H1	O16	N14	Ca	C	Si
H20	0.667	0.333	--	--	--	--
Air	--	0.211	0.784	0.005	0.000	--
Acrylic	0.533	0.133	--	--	0.333	--
Quartz Mat. + Acrylic Resin	0.532	0.135	--	--	0.332	0.001

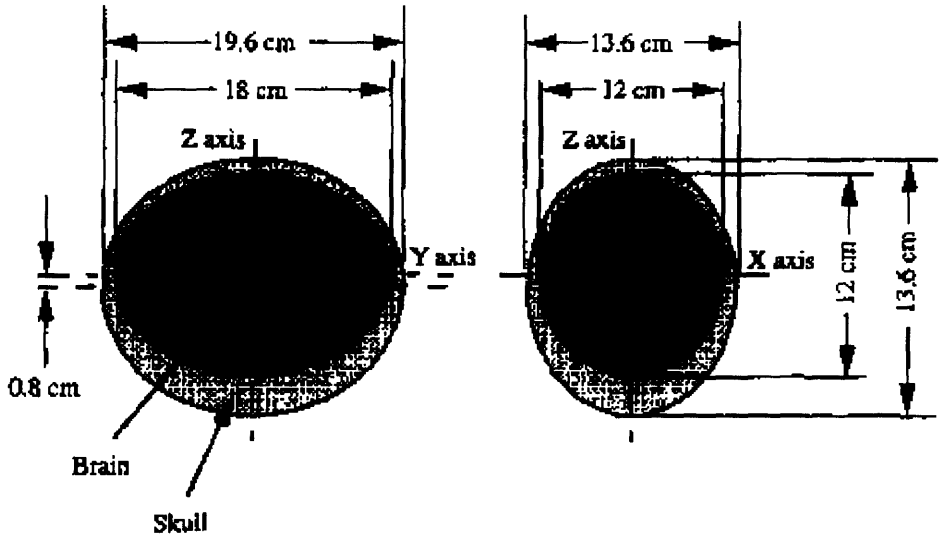

Figure 1: A drawing of the Deutsch and Murray model of the head and brain using ellipsoids for the inner and outer surfaces of the skull [3]

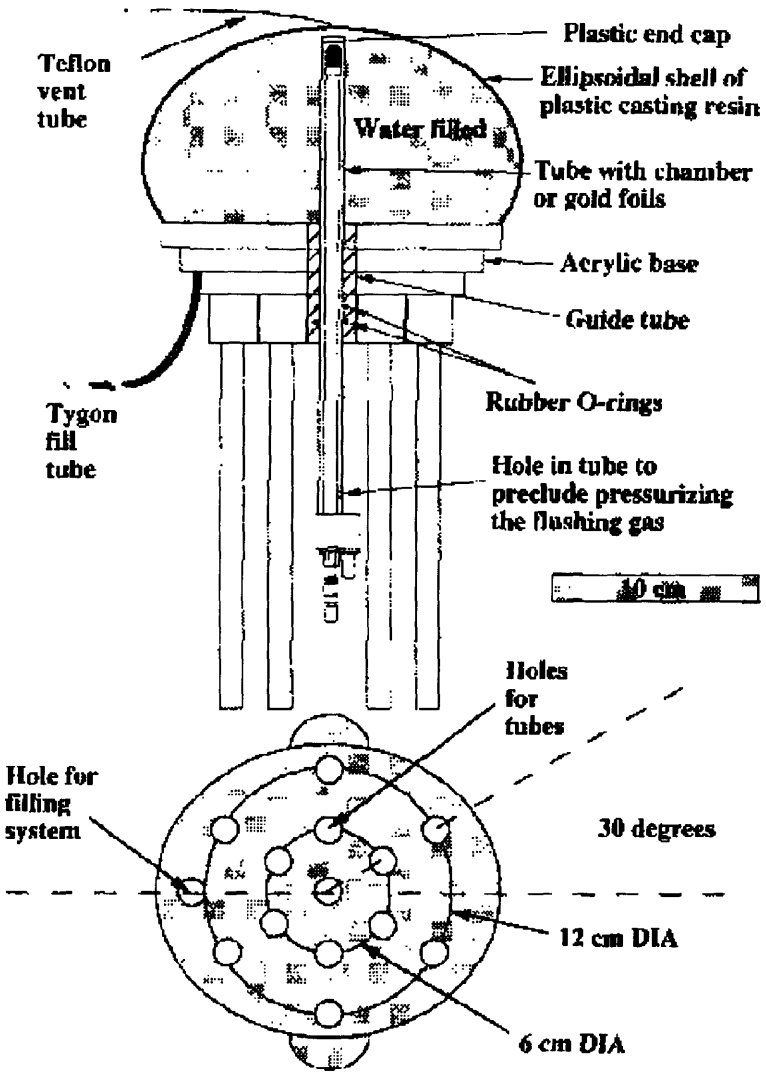

Figure 2: Side and bottom view of the ellipsoidal water-filled head phantom showing how detectors and activation foils can be inserted in hollow tubes into the internal water volume [3]

The phantom routinely used for dosimetry measurements at BNL was a solid Lucite cube. The Lucite cube has dimensions 14 cm x 14 cm x 14 cm (total volume of 2744cm^3) and the composition is defined as 8% H, 60% C, and 32% N by weight. This cube has a hole in the front face that extends down the centerline of the cube, as well as off-axis holes, to accommodate various Lucite rods of 1.59 cm diameter. Slits are cut in the rods at 3.5, 7.0, and 10.5 cm from the front face of the phantom, allowing for measurements to be made at these depths by TLDs that can be placed in the slits. Rods containing Au foils or Cd capsules with Au foils in them can also be placed in the Lucite

cube for additional measurements. For thermal neutron flux measurements, these slits can hold either a bare Au foil or a cadmium capsule in which an Au foil is placed. The Au foils are square shaped and weighed between 3.02 ± 0.03 and 25.59 ± 0.26 mg [1]. Additionally, for gamma dose measurements or fast neutron dose measurements, an ion chamber can be inserted instead of the Lucite rod, and can be located at a desired depth by using spacers. To make measurements at additional depths, slits were created at 1.0, 2.0, 5.0, and 9.0 cm. For this study, the Lucite cube phantom was placed with its front face touching the patient collimator, and its central axis aligned with the beam axis [1]. A diagram of the Lucite cube can be seen in Figure 3.

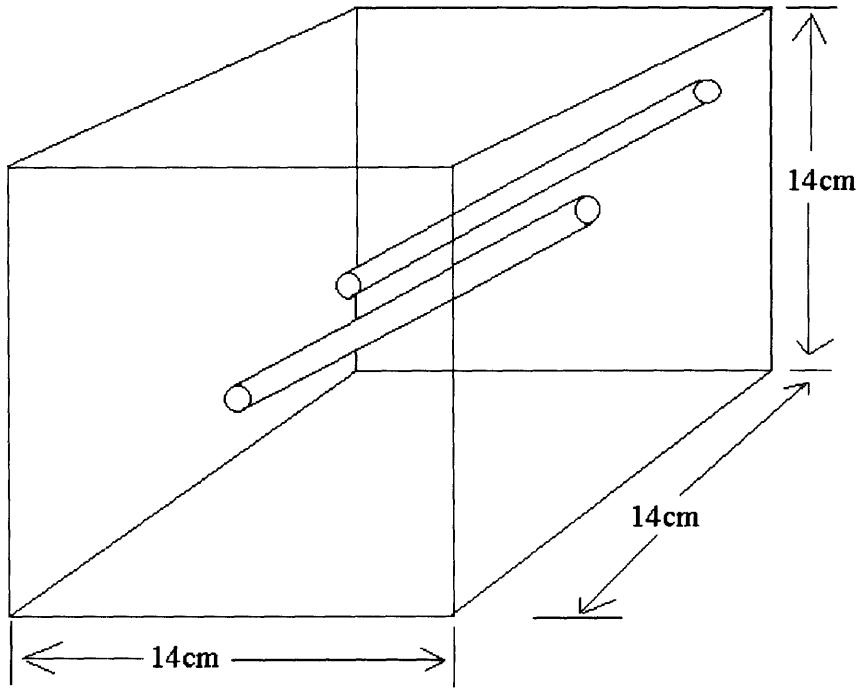

Figure 3: Diagram of 14cm x 14cm x 14cm BNL Lucite cube phantom

2. Dosimetry methods

For the BNL/MIT dosimetry intercomparison, measurements were performed by MIT researchers in the BNL beam with the 12-cm collimator in place using both the MIT ellipsoidal head phantom and the BNL Lucite cube. Data are available in the Lucite cube from BNL using both the original 8-cm collimator, as well as the 12-cm collimator, which was installed in 1996 [2]. Since the MIT measurements were performed only with

the 12-cm collimator in place, a comparison of the BNL beam with the 8-cm collimator cannot be performed at this time.

MIT researchers measured each beam component in December of 1997 and again in July and September of 2000. Measurements were performed in the Lucite cube and the ellipsoidal phantom for gamma dose, thermal neutron flux, and fast neutron dose. In-air fast neutron dose measurements were also performed.

a. MIT gamma and fast neutron doses

Photon and fast neutron dose rates were measured in the Lucite cube phantom as well as in-air using the dual chamber technique of Attix [4]. This technique involves using two chambers: one that is neutron sensitive and one that is neutron insensitive. Using the neutron insensitive chamber, the photon dose rate can be measured. The neutron-sensitive chamber measures both gamma and fast neutron dose. Once these measurements are known, the data from the neutron-insensitive chamber can be subtracted from the data obtained from the neutron-sensitive chamber to determine the neutron dose rate. The neutron sensitive chamber used by MIT is a 2.51 mm-thick A-150-walled, muscle tissue-equivalent, ionization chamber (IC-18 Far West Technology) that has an active volume of 0.1 mL and is flushed with tissue-equivalent gas (64.4% CH_4, 32.4% CO_2, and 3.2% N_2) at a rate of 20mL/min [1, 5]. The neutron-insensitive chamber used by MIT is similar but has a 1.65 mm-thick wall made of graphite and is flushed with CO_2 gas. Both chambers are operated with an applied voltage of +250 V and have calibration certificates traceable to the National Institute of Standards and Technology (NIST) [1, 5]. In-air measurements were also performed with the chambers located along the central axis of the beam: the plane that defines the exit end of the patient collimator. Overall uncertainties of about 9.0% are associated with the MIT photon dose rate measurements [1, 5]. For the fast neutron dose rate measurements, overall uncertainties in the Lucite cube are about 32.5% at a depth of 1 cm, and of 100% at 4 cm and deeper, and uncertainties in-air are about 17% [1, 5]. In-phantom gamma and fast neutron dose were made at 1 cm depth increments from 1 cm to 11 cm depth.

b. MIT thermal neutron flux

Thermal fluxes were determined using the cadmium difference technique. Au foils of thickness 0.005 cm were used with 0.051 cm-thick Cd covers. Bare foils were irradiated

at the surface of the phantom and at depths of 1 cm increments up to 8.0 cm, as well as at 10.0 cm and 12.0 cm. To minimize thermal flux suppression, the Cd-covered foils were irradiated at the surface of the phantom and at depths with 2-cm increments up to 10.0 cm. MIT assumes that the thermal neutron activation occurs solely due to neutrons with a velocity of 2200 m/s and have an absorption cross section of 98.8 barns [1].

Once the Au foils were activated, they were measured at MIT using a high-purity germanium (HPGe) detector that had been energy-and-efficiency-calibrated using a Standard Mixed Radionuclide Source (SRM 4275C-45) from NIST [1, 5]. This source consists of a thin deposit about 0.6 cm in diameter on a polyester tape, and reproduces the geometry of a Au foil. It is placed about 13 cm away from the face of the detector to minimize coincidence-summing errors. Overall uncertainties of about 7.4% are associated with the MIT thermal neutron flux measurements [1, 5].

c. BNL gamma and fast neutron dose rates

BNL researchers used the mixed-field ionization chamber dosimetry technique, based on the methodology of Attix [4] for both gamma and fast neutron absorbed dose measurements in air. This technique is the same as the one used by MIT, with one neutron sensitive and one neutron insensitive ionization chamber. Both chambers are the same as those used by MIT. Both chambers were calibrated at Far West Tech., Inc. by ^{137}Cs source irradiation [2]. They were covered with ^{6}LiF thermal neutron shields made by two 0.0794 cm-thick cellulose acetate butyrate cylindrical tubes, separated by ~4 mm thick ^{6}LiF (~95% enriched isotopic ^{6}Li) compressed powder and sealed at each end [2].

BNL measured gamma absorbed dose rates in the Lucite cube phantom by using LiF-700 thermoluminescent dosimeters (TLDs) (Harshaw Chemical Company, Solon, Ohio [2]). These TLDs are made of lithium fluoride, 99.93% enriched in ^{7}Li, and are about 1mm x 1mm x 6mm. Unfortunately, they do contain small amounts of ^{6}Li, which responds strongly to thermal neutrons in the phantom. Because of this, each batch of TLDs was calibrated for thermal neutron response at the Brookhaven Medical Research Reactor's Thermal Neutron Irradiation Facility. The TLDs were calibrated for gamma dose response in a calibrated ^{60}Co source at BNL [2]. The TLD rods were covered with a 2 mm thick ^{6}Li metal shield to measure the absorbed dose from gamma rays in the beam at the irradiation aperture. The uncertainty in the measured photon dose rates is about

10% [2]. The uncertainty in the fast neutron dose measurements in air is about 15% [2]. BNL researchers did not perform fast neutron measurements in the Lucite cube. Instead, they relied on the in-air surface fast neutron measurement and calculations to generate fast neutron depth-dose information.

d. BNL thermal neutron flux

BNL performed measurements to determine thermal and epithermal neutron fluence rates, gamma dose rates, and fast neutron dose rates either in air or in the Lucite cube phantom. Bare and cadmium-covered Au foils 0.00127 cm thick and with an average diameter of 0.8 cm were used to measure thermal neutron fluence rates. However, instead of using an HPGe detector to measure the activated foils as MIT did, BNL used a NaI(T1) well-type detector to measure the Au foil activation. Calibration sources were obtained from DuPont, and satisfied NIST standards [2, 6]. Uncertainty in the BNL-measured thermal neutron fluence rates in both collimators is about 6% [2].

BNL assumes that thermal neutron activation occurs due to neutrons with a range of energies. BNL calculates the energy distribution for thermal neutrons at each depth in the phantom and determines an effective cross section associated with each position. They calculated cross sections of 80.0, 83.0, and 86.0 barns at depths of 3.5, 7.0, and 10.5 cm, respectively [1]. This is different from the MIT definition of thermal neutrons, and therefore when making a thermal neutron comparison, the fluxes cannot be directly compared. However, when thermal neutron dose is calculated from the measured flux, the difference caused by these different thermal neutron definitions disappears due to the different kerma factors associated with the different cross sections.

e. Routine BNL dosimetry measurements in the Lucite cube

Beam measurements were performed by BNL on a monthly basis in the Lucite cube at 3.5, 7.0, and 10.5 cm, between 1994 and 1999 as part of the BNCT clinical trial quality control program. Figure 4 shows the photon dose and thermal neutron flux measurements at 3.5 cm versus the date on which those measurements were taken. The uncertainty in the experimental measurements over a one-year period of time in the 8 cm collimator was about 5% [2]. The dosimetry methods used to obtain these measurements are as described above. Between February 7, 1996 and March 27, 1996, a new collimator was put in place at the BMRR. This new collimator was 12 cm in diameter and 7.6 cm

thicker than the former 8-cm-diameter collimator. There is a clear decrease in thermal neutron flux and gamma dose rate at this point. The thermal neutron flux decreases on average by about 23% and the gamma dose rate decreases on average by about 34%. This is due to the fact that while the 12-cm collimator has a larger neutron source area, it is offset by the decrease in flux caused by the longer beam path (since the 12-cm collimator is 7.6 cm longer than the 8-cm collimator). At the peak, the thermal neutron flux decreases by 18% at 3MW power [2]. Additionally, some of the fuel rods were shuffled between 2/10/98 and 3/12/98. The effect of this core shuffle can be observed in both graphs by about a 15% increase in photon dose rate and 11% increase in thermal neutron flux. When applying these changes to the RTPE source files, it was discovered that the increase in flux and gamma dose rate after the core shuffle yielded an insignificant change in the prescribed dose to the patient. Because of this, only three treatment plans in the BNL clinical trial made use of a separate source definition after 2/10/98. All subsequent treatment plans used the source definition used before the core shuffle. This means that two different source definition files were used to calculate the treatment plans for these two groups of patients: those treated before and those treated after the new collimator was put in place. Since MIT measurements were only performed when the 12 cm collimator in place, all evaluation of adjustment factors will be determined for this group. Without having the MIT measurements with the 8 cm collimator, it is impossible to know whether or not two different sets of adjustment factors should actually be applied to the patients. Thus, the adjustment factors calculated below for the 12 cm collimator are used for all BNL patients.

All calculations in this thesis were performed specifically to compare the MIT clinical trial to the BNL clinical trial. Access was available to all original patient treatment planning information from both the BNL and MIT clinical trials, as well as to the original computer used at BNL to run patient treatment plans using RTPE. It was important to rerun patients treated at BNL on the BNL software because this would eliminate possible errors associated with differences in treatment planning software. Particularly when rerunning patient treatment plans, the original files (source, input, material, cross section, etc) were used, and only one or two parameters were changed at a time, which allows for the effect of these individual parameters on the treatment plans to be seen.

With this information, a direct comparison of MIT measurements and BNL RTPE output in the Lucite cube and the ellipsoidal head phantom can be performed. This will allow for a calculation of the scaling factors that must be applied to all the BMRR dose components so that they match MIT measurements. Ultimately, these scaling factors can be applied to the BNL patient data, and a combined analysis of patient brain doses at MIT and BNL can be achieved.

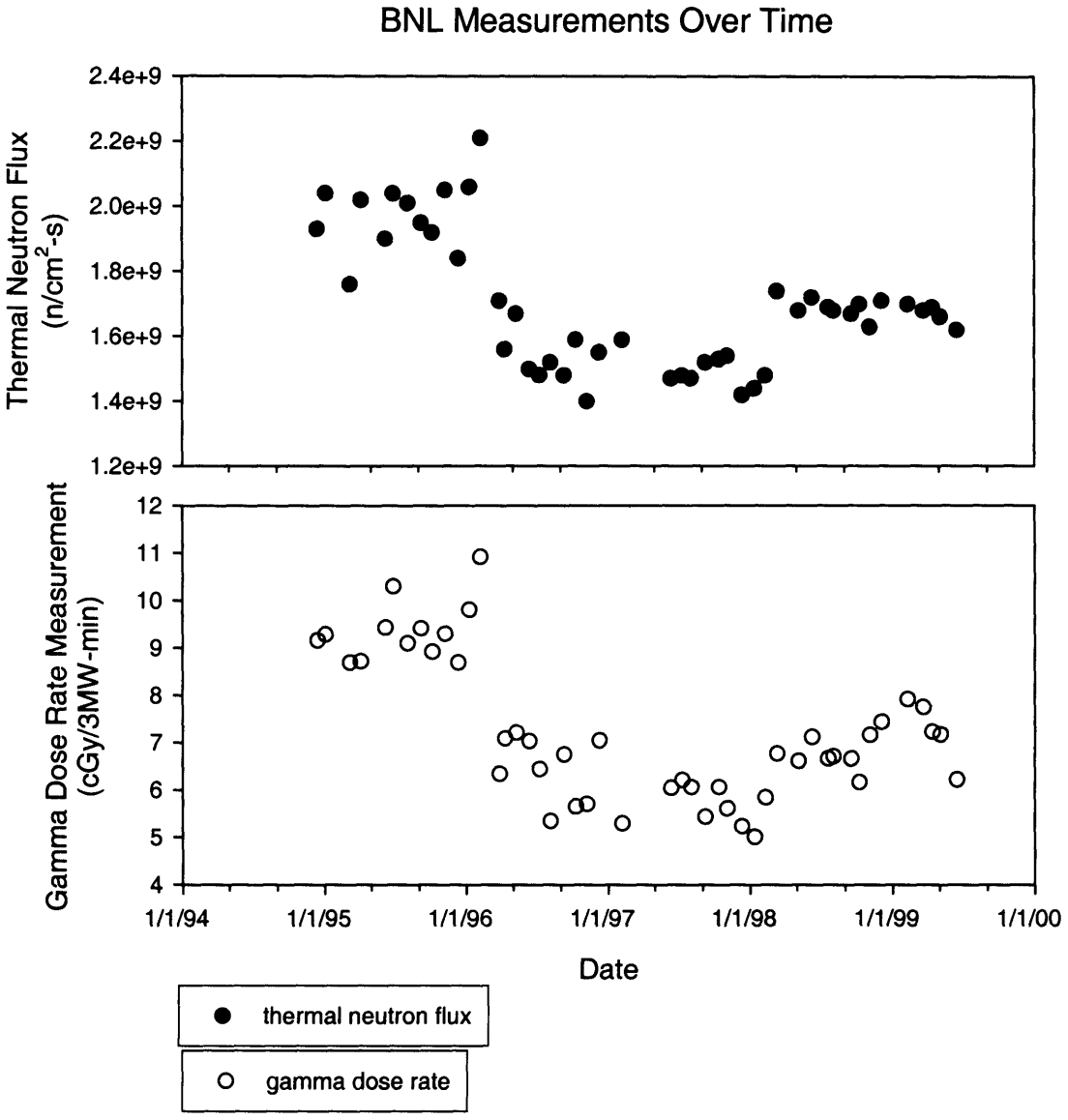

Figure 4: Results of the routine gamma dose rate (bottom) and thermal neutron flux measurements (top) performed by BNL from December 1994 to June 1999 [7]

References:

1. K.J. Riley, P.J. Binns, D.D. Greenberg, O.K. Harling, A physical dosimetry intercomparison for BNCT, Med. Phys., **29:** 898-904 (2002).

2. H.B. Liu, D.D. Greenberg, J. Capala, An improved neutron collimator for brain tumor irradiations in clinical boron neutron capture therapy, Medical Physics, **23:** 2051-2060 (1996).

3. O.K. Harling, K.A. Roberts, D.J. Moulin, R.D. Rogus, Head phantoms for neutron capture therapy, Medical Physics **22:** 579-583 (1995).

4. F.H. Attix, Introduction to Radiological Physics and Radiation Dosimetry, John Wiley & Sons Inc., New York, 1986.

5. R.D. Rogus, O.K. Harling, J.C. Yanch, Mixed field dosimetry of epithermal neutron beams for boron neutron capture therapy at the MITR-II research reactor, Med. Phys., **21:** 1611-1625 (1994).

6. Liu, H. B., Brugger, R. M., A study of the concept of a fission plate as a source for an epithermal neutron beam, In: Proceddings of the Sixth International Symposium of Neutron Capture Therapy, 10/31-11/5, (1994).

7. D. Greenberg, unpublished data

III. Differences in ^{14}N Concentration

There is no standard reference that all centers must follow when defining tissue composition, and therefore during the BNCT clinical trials, different centers used different brain compositions, particularly ^{14}N weight percent. The recommended values changed over the years (as well as different values being recommended by different groups), however the clinical centers treating patients with BNCT chose for themselves whether or not to change the ^{14}N values they used according to these recommended values. For instance, while both MIT and BNL originally used a value of 1.8 weight percent ^{14}N for many years, MIT currently uses a value of 2.2 weight percent, as does Petten. ICRU 46 defined normal brain as having 1.8% ^{14}N [1]. These two percentages are the two extremes of the ^{14}N values used in BNCT. When attempting to pool the patient data, the question arose as to what effect this difference in composition would make in the ultimate definition of dose given to the patient, and what adjustment would need to be made to patient treatment plans in order to compare patient data from an institution using a nitrogen weight percent of 1.8% to one using 2.2%. By evaluating these differences, a determination can be made as to whether or not a correction needs to be made to BNL doses and RTPE output to match doses that would be as measured by MIT in the same phantom.

The dose received by the patient during treatment is comprised of several different components: a gamma component (from gamma rays in the neutron beam and a larger component from the hydrogen capture reaction), a ^{14}N dose component from the nitrogen capture reactions in tissue (which creates a 615 keV proton), a fast neutron component (from proton recoils produced by fast neutrons colliding with hydrogen in tissue), and a boron-10 component (which is another thermal neutron dose and is proportional to the amount of ^{10}B in the tissue). The dose-depth distribution of each of these components in a Lucite cube, containing no ^{10}B, obtained from RTPE in the BNL beam can be seen in Figure 5. The doses for this figure were calculated as the dose to normal brain tissue. All doses stated in this thesis are calculated at a reactor power of 3MW.

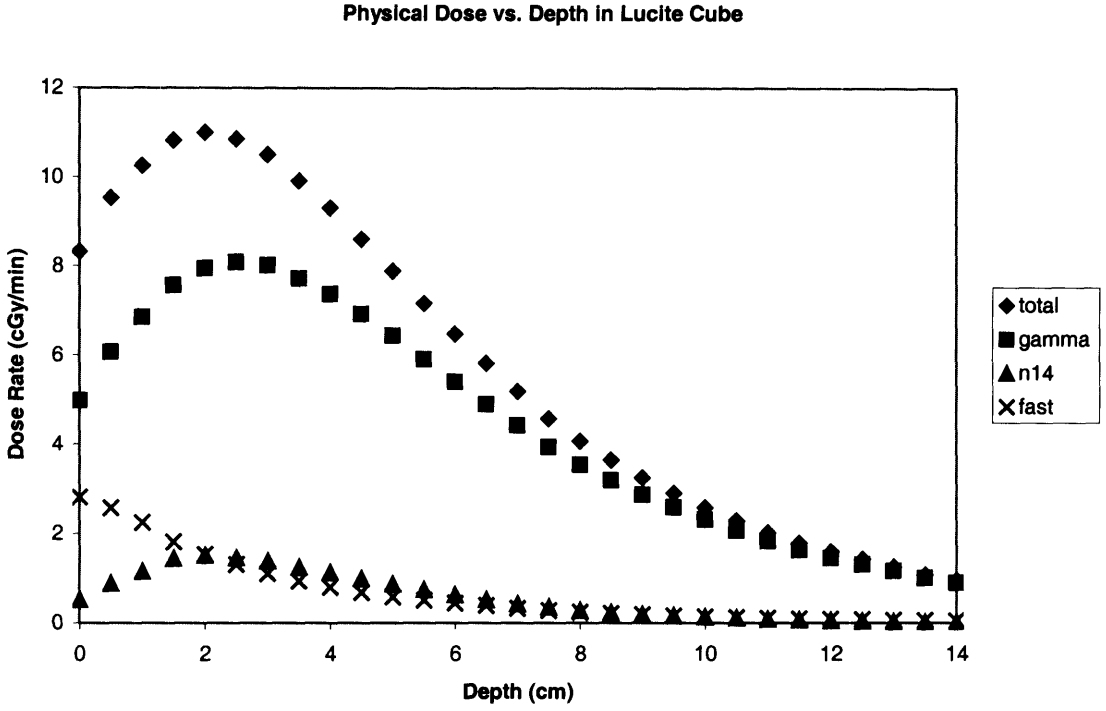

Figure 5: Depth-dose profile in Lucite cube (with no boron) for all components, using 12 cm collimated source as calculated with RTPE

Table 3 shows the material definition of normal brain in RTPE with only the natural concentration of boron in blood (which is almost zero). Table 4 shows the definition of normal brain tissue as defined by ICRU 46 and MIT in 2002 [1, 2]. As can be seen from Figure 5, the ^{14}N dose is only a small contributor at all depths. It is in fact typically less than 13% of the total dose at all depths. This is because ^{14}N makes up such a small fraction of normal brain tissue, and the fraction of the total dose that is from the ^{14}N reaction will depend on the weight percent ^{14}N in tissue.

Table 3: Material definition for normal brain in RTPE [3]

Material	Atom Density (atoms/barn-cm)	Wt %
H	6.663E-02	10.57
O	2.886E-02	73.27
C	4.742E-03	9.03
N	8.283E-04	1.84
B	4.402E-09	0.00
Na	3.840E-05	0.15
Cl	5.340E-05	0.30
K	6.289E-05	0.39
P	7.939E-05	0.39

Table 4: Normal brain composition as defined by ICRU 46 [1] and by Harvard-MIT, as of 2002 [2]

Element	ICRU 46 weight %	Harvard-MIT weight %
H	10.7	10.57
C	14.5	13.94
N	2.2	1.84
O	71.2	72.59
Na	0.2	0
Mg	0	0
P	0.4	0.39
S	0.2	0
Cl	0.3	0.14
K	0.3	0.39
Ca	0	0
Density (g/cm^3)	1.04	1.047

The first step in comparing the effect of ^{14}N differences on patient doses at BNL or Harvard-MIT is to make changes to a simple common phantom. In this case the 14cm x 14cm x 14cm Lucite cube containing no boron was chosen. While the particle transport takes place through the material defined as Lucite (see Table 5), the dose is calculated in normal brain tissue (see Table 3). The ^{14}N weight percent in normal brain tissue can be changed in the RTPE input file and the effect of this change on the calculated total dose rate can be observed. By making the necessary material definition changes in RTPE and

keeping all other input the same, the user is able to determine what effect changing the nitrogen concentration has on the calculated dose to tissue.

Table 5: Material definition for Lucite as defined in RTPE

Material	Atom Density (atoms/barn-cm)
H	0.05777
O	0.01444
C	0.03511

With a nitrogen concentration of 1.8% (i.e., the BNL model), the nitrogen depth-dose profile in the cube in the BNL beam is shown in the bottom curve in Figure 6. With a nitrogen concentration of 2.2% (i.e., the MIT model), the nitrogen depth-dose profile in the cube in the BNL beam is shown in the top curve in Figure 6. Figure 7 shows the effect that varying the nitrogen concentration has on the total dose, which is the more relevant parameter from a clinical point of view. This graph shows the total dose with no boron present. As is clear from this graph, the difference between the two total doses is very small. In fact, the two numbers are within 3% everywhere, including at the peak. As mentioned before, the ^{14}N dose comprises only a small percent of the total dose. Because the other dose components (which can be seen in Figure 5) comprise a more significant portion of the total dose, a small change in a component that makes up less than 13% of the total dose will lead to an even smaller change in the total dose. Additionally, this analysis included no boron in the normal tissue. Once the boron component is added back in, the ^{14}N component will comprise an even smaller percent of the total dose, and the effect of changing this dose component will be even smaller. Figure 8 shows a comparison of the ^{14}N dose and the total dose in the Lucite cube for tissue composition of both 1.8% and 2.2% ^{14}N.

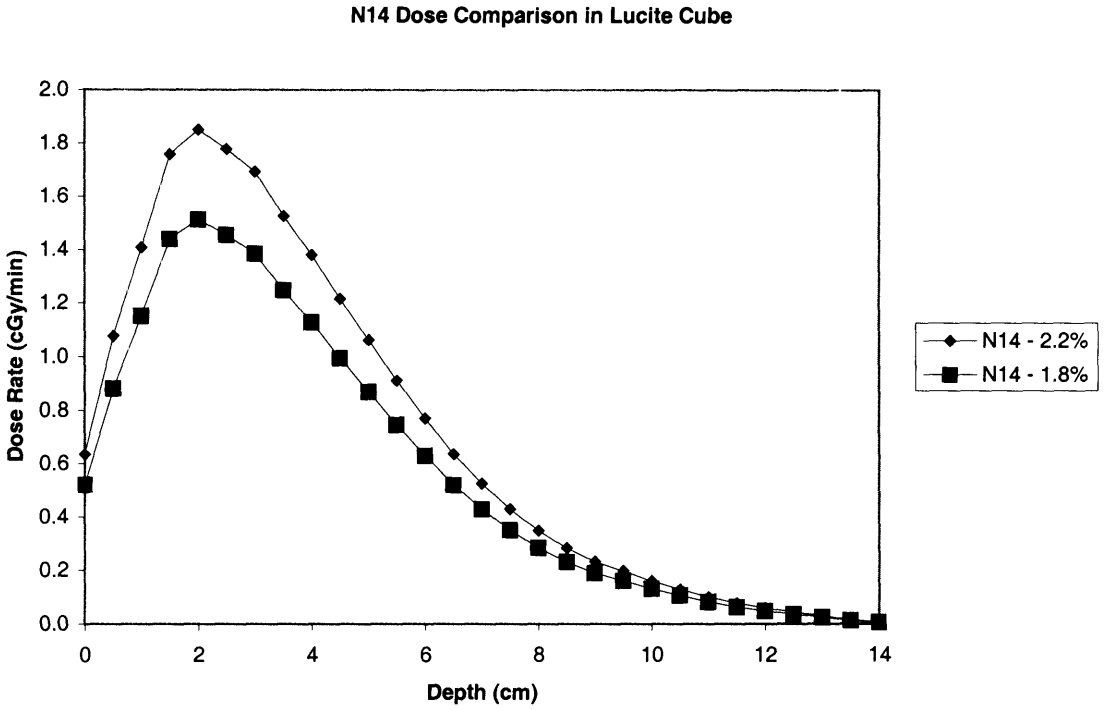

Figure 6: ^{14}N dose rates in the Lucite cube with no ^{10}B, with nitrogen concentrations of either 1.8% or 2.2%

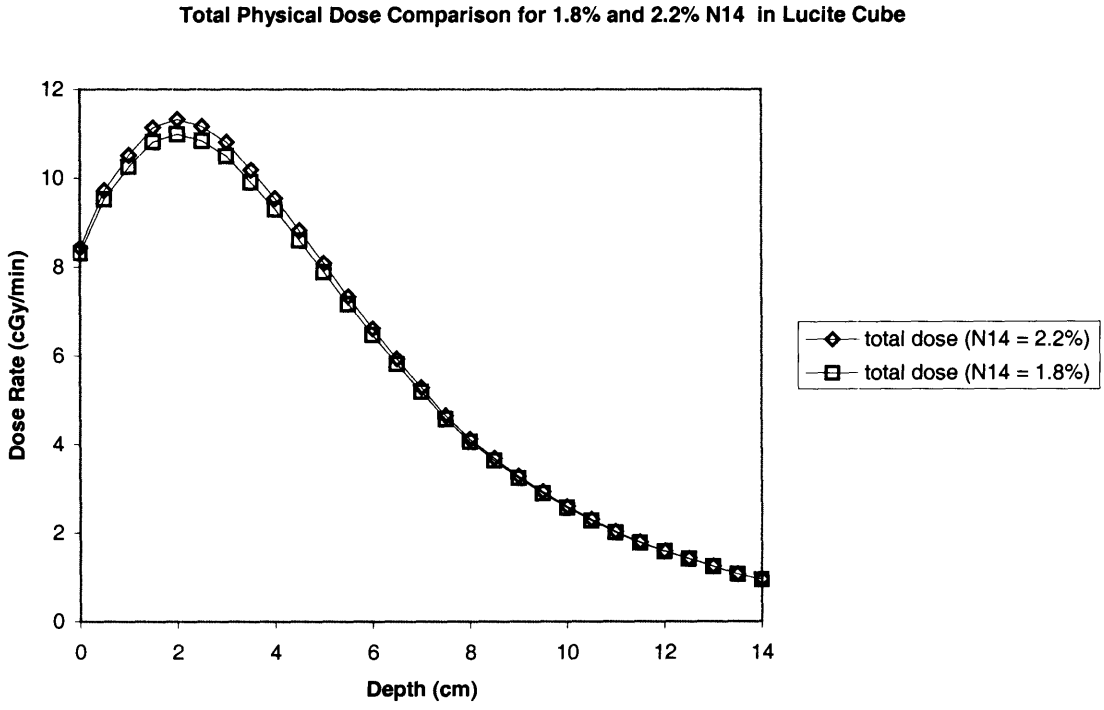

Figure 7: Comparison of total dose rates in the Lucite cube with no ^{10}B, with nitrogen concentrations of either 1.8% or 2.2%

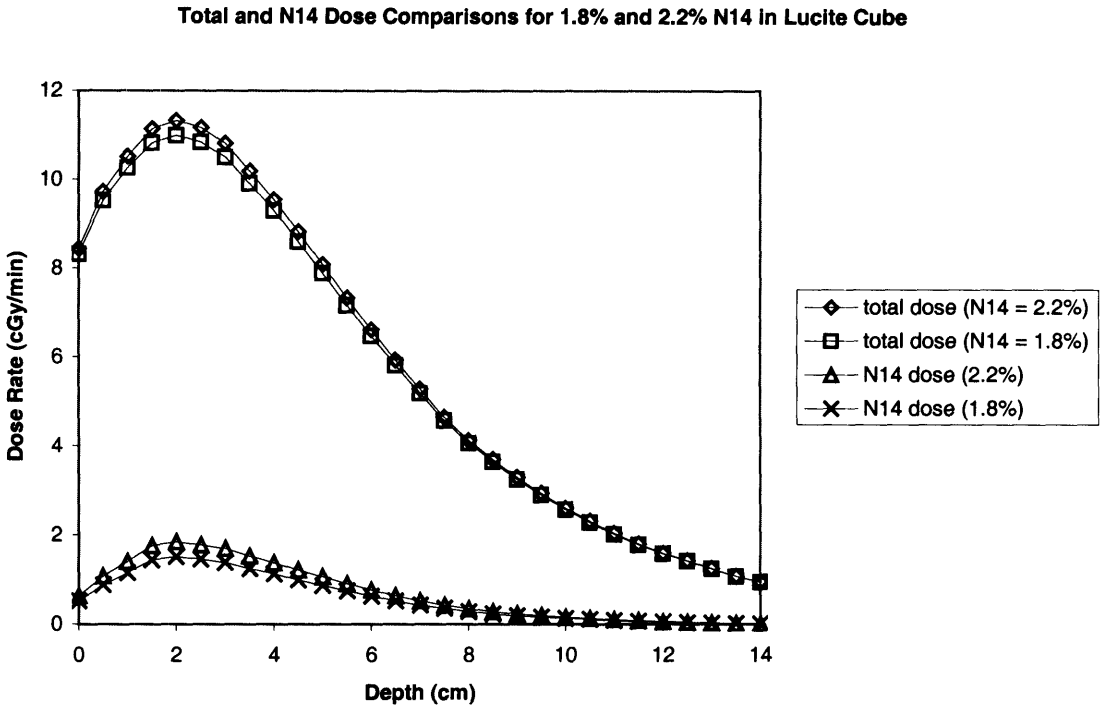

Figure 8: Depth-dose profiles of both the ^{14}N dose rates and the total dose rates in the Lucite cube with no ^{10}B, for nitrogen concentrations of either 1.8% or 2.2%

The results obtained from the Lucite cube indicate that the difference in peak dose received by the patient due to differences in tissue nitrogen composition will be negligible. However, to check this hypothesis, it is important to examine a sample patient treatment plan, to be sure that the effect seen in the Lucite cube is representative of that seen in a patient. Figure 9 shows the comparison of the ^{14}N dose for a representative 1-field patient treatment plan run with both 1.8% ^{14}N in tissue and 2.2% ^{14}N in tissue. The comparison of the total dose can be seen in Figure 10, along with the ^{14}N dose. The peak dose for the 1-field patient is changed by less than 3%, and the total dose actually changes by less than 3% everywhere along the curve. The 'normal brain' for this patient was assumed to have a blood boron concentration of 10 μg $^{10}B/g$. Almost all patients treated in the BNL and MIT clinical trials had blood-boron concentrations of between 10 and 20μg/g.

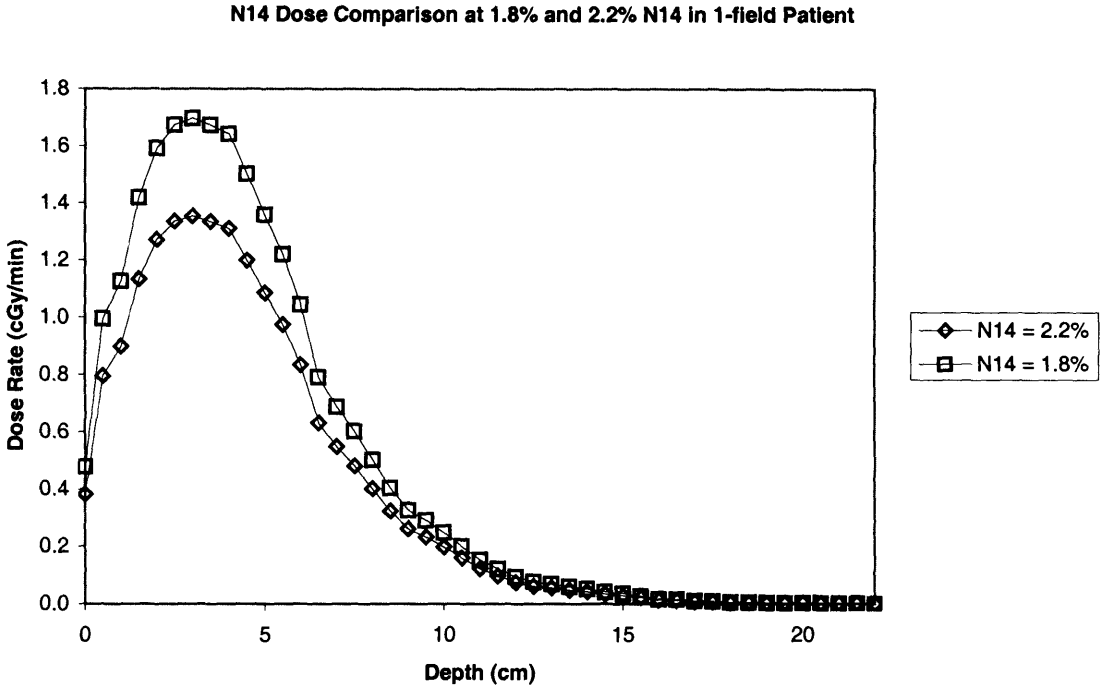

Figure 9: ^{14}N dose rate comparison for a 1-field BNL patient with either 1.8% or 2.2% nitrogen in normal brain tissue using the 12-cm collimator

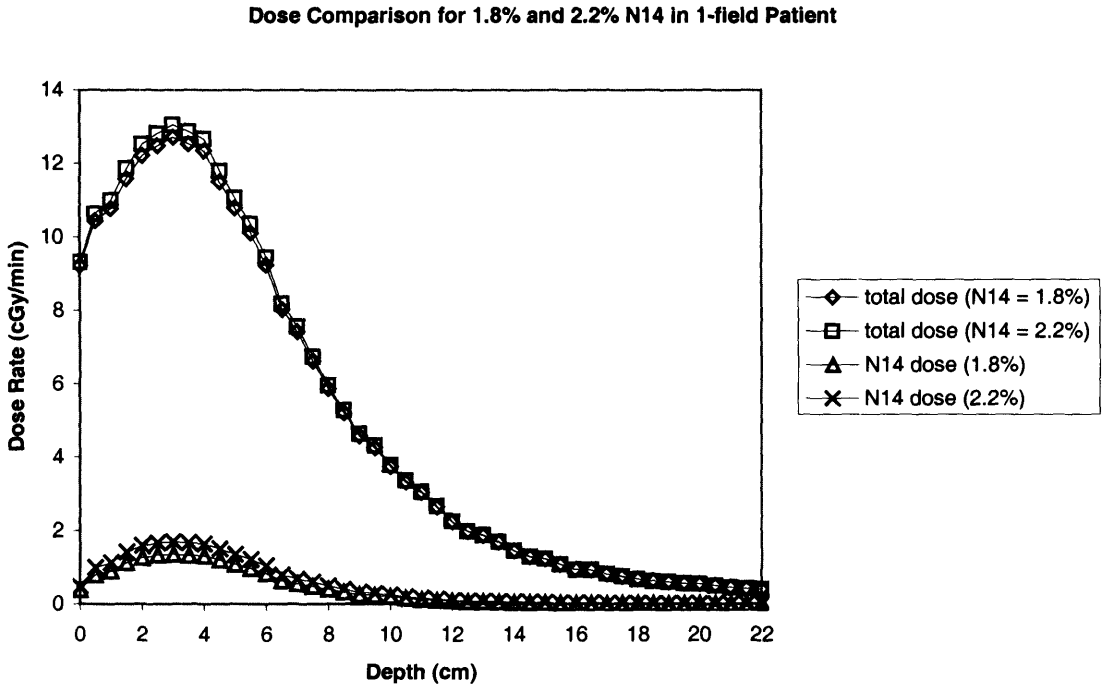

Figure 10: Total and ^{14}N dose rate comparison for a 1-field BNL patient with either 1.8% or 2.2% nitrogen in normal brain tissue using the 12-cm collimator

The dose administered to normal tissue is dependent upon the amount of ^{14}N found in the tissue. While different clinical centers use slightly different definition for the percent composition of ^{14}N in normal brain tissue, it is clear that the effect this difference has on the total prescribed dose is negligible. Therefore, it is safe to say that a direct comparison between BNL patient doses and MIT patient doses can be performed without the need of any sort of scaling factor to account for the change in tissue nitrogen composition.

References:

1. ICRU 46: Photon, electron, proton and neutron interaction data for body tissues, 1992

2. M.R. Palmer, T. Goorley, W.S. Kiger III, P.M. Busse, K.J. Riley, O.K. Harling, R.G. Zamenhof, Treatment planning and dosimetry for the Harvard-MIT Phase I clinical trial of cranial neutron capture therapy, International J. Radiation Oncology Biol. Phys., **53:** 1361-1379 (2002).

3. D.W. Nigg, F.J. Wheeler, D.E. Wessol, J. Capala, M. Chadha, Computational dosimetry and treatment planning for boron neutron capture therapy, J. Neuro-Oncol. **33:** 93-103 (1997).

IV. Comparison of Patient Dose Component Measurements in the BNL Beam by BNL and MIT

In order to pool BNCT patient data from the various BNCT facilities, a direct comparison of the dose administered to patients by two facility's neutron beams must be made. To do this, an assessment of each facility's measurement techniques must be performed. Every BNCT facility's neutron beam is unique in its dose component make-up, and each component must be compared individually. For this evaluation, two different phantoms will be used: the Lucite cube phantom routinely used by BNL, and the ellipsoidal water-filled head phantom routinely used by MIT. These phantoms were both simulated in RTPE using both a combinatorial geometry (CG), as well as geometry reconstructed from CT images and compared to measurements in the actual phantoms. A comparison of the CT to the CG geometry in each phantom showed that the same results could be obtained regardless of geometry, and therefore all results will show the CG geometry output. While the Lucite cube is the simplest geometry, it may actually be too simple to rely upon for good results due to the fact that it does not closely resemble any aspect of a potential patient to be treated with BNCT. Since the shape of the ellipsoidal head phantom is more representative of an actual patient, it will therefore serve as a good check of the accuracy of the model created from the Lucite cube.

1. Error Analysis of MIT & BNL Measurements

Before proceeding to examine the difference between the MIT and BNL dose measurement techniques, it is necessary to examine the doses measured and published by each group more closely [1, 2]. All of the BNL and MIT measurements have errors associated with them (from measurement error, errors associated with the detectors, etc.). These errors depend on number of counts in the detector and properties of the detector itself, among others. It is important to fully understand these errors before doing further evaluation.

Table 6 and Table 7 detail the measurements made by MIT and BNL in the BMRR epithermal neutron beam with either the 8-cm collimator or the 12-cm collimator. These measurements were all made in the Lucite cube phantom. The MIT measurements were

performed in September 2000, and Ben Liu et al performed the BNL dose measurements in 1996 [2]. The monthly quality control dosimetry measurements detailed previously are in good agreement with the published BNL measurements [2, 3].

Table 6: MIT-measured dose rates, thermal neutron flux, and calculated ^{14}N dose rates in Lucite cube in the BMRR at a reactor power of 3MW with the 12-cm collimator (September 2000) [1]

Depth in Cube (cm)	Gamma Dose Rate (cGy/min)	Fast Dose Rate (cGy/min)	Thermal Flux $(cm^{-2}s^{-1})*10^8$	^{14}N Thermal Dose (calculated) (cGy/min)
1.0	4.84±0.44	2.38±0.70	--	--
2.0	5.62±0.51	2.00±1.00	--	--
3.5	5.76±0.52	1.25±1.00	13.73±1.02	1.10±0.08
5.0	4.93±0.44	0.36±035	--	--
7.0	3.75±0.34	0.38±0.37	4.88±0.36	0.39±0.03
10.0	1.60±0.14	--	--	--
10.5	1.29±0.12	--	1.13±0.08	0.09±0.01

Table 7: BNL-measured dose rates, thermal neutron flux, and calculated ^{14}N dose rates in Lucite cube in the BMRR at a reactor power of 3 MW with the 8-cm and 12-cm collimator [2]

Depth in Lucite Cube (cm)	8-cm collimator Gamma Dose Rate (cGy/min)	8-cm collimator Thermal Flux $(cm^{-2}s^{-1})*10^8$	8-cm collimator ^{14}N Thermal Dose (calculated) (cGy/min)	12-cm collimator Gamma Dose Rate (cGy/min)	12-cm collimator Thermal Flux $(cm^{-2}s^{-1})*10^8$	12-cm collimator ^{14}N Thermal Dose (calculated) (cGy/min)
3.5	4.71±0.47	19.4±1.2	1.56±0.10	3.87±0.39	15.9±1.0	1.279±0.080
7.0	2.5±0.25	6.41±0.38	0.516±0.031	2.45±0.25	5.7±0.34	0.459±0.027
10.5	1.28±0.13	1.53±0.09	0.123±0.007	1.27±0.13	1.38±0.08	0.111±0.006

Measurements were also taken in the BNL beam by MIT in the ellipsoidal head phantom. Unfortunately, equivalent measurements were not performed by BNL in the same phantom. However, the MIT measurements in the head phantom will be useful as a check on the accuracy of the scaling factor results obtained later in this thesis. The MIT measurements in the ellipsoidal head phantom are detailed in Table 8.

Table 8: MIT-measured dose rates, thermal neutron flux, and calculated 14N dose rates in the ellipsoidal head phantom in the BMRR epithermal neutron beam at a reactor power of 3 MW with the 12-cm collimator [1]

Depth in Lucite cube (cm)	Gamma Dose Rate (cGy/min)	Thermal Neutron Flux ($cm^{-2}s^{-1}$)*10^8	^{14}N Thermal Dose (calculated) (cGy/min)
1.00	5.55±0.40	12.2±0.6	2.02±0.10
2.00	6.05±0.40	14.6±0.8	2.42±0.13
3.00	6.20±0.35	14.0±0.8	2.32±0.13
4.00	5.90±0.30	12.0±0.7	1.99±0.12
5.00	5.40±0.25	9.30±0.6	1.54±0.10
6.00	4.55±0.25	7.00±0.4	1.16±0.07
7.00	4.00±0.20	--	--
8.00	3.50±0.20	3.20±0.1	0.53±0.02
9.00	2.85±0.10	--	--
10.00	2.50±0.08	1.50±0.1	0.25±0.02
11.00	2.00±0.05	--	

a. MIT measurement errors

The thermal flux was measured directly at a reactor power of 3MW in the solid Lucite cube phantom by gold foil activation analysis [1]. With this flux value known, the ^{14}N and ^{10}B doses can be calculated by (assuming kerma coefficients for ^{14}N and ^{10}B of $0.745*10^8$ and $8.66*10^{-6}$ cGy-cm^2, respectively):

$$D_{N14} = (44.7 * 10^{-9})F_n\phi \quad \text{in cGy/min} \qquad \text{(Eq. 1, [4])}$$

$$D_{B10} = (5.196 * 10^{-4})F_b\phi \quad \text{in cGy/min} \qquad \text{(Eq. 2, [4])}$$

Where,

F_n = the fraction by weight of the nitrogen in tissue = 1.8%

F_b = the fraction by weight of the ^{10}B in tissue $\approx$ 10-20μg/g

ϕ = the thermal neutron flux in neutrons/cm^2s

Average ^{10}B concentrations in the BNCT patients were typically between about 10 and 20μg/g, and therefore these values were used to calculate the minimum and maximum ^{10}B dose rates to get an idea of the range of doses from ^{10}B. The gamma dose was measured by MIT directly in the cube in the manner described previously.

As can be seen from Table 6, the errors on the fast neutron measurements in the Lucite cube are very large. Fast neutron doses in the cube were calculated using an A-150 plastic walled ionization chamber, subtracting for the photon and thermal neutron responses. Because the photon dose in the cube is higher than the photon dose in air, the

error when measuring fast neutron dose in the Lucite cube is larger than measuring the same way in air (greater subtraction is necessary in the cube, which allows for greater error in the fast neutron measurement). Therefore, when calculating the total dose, it would be more accurate to use the fast neutron measurement in air and scale the RTPE fast neutron curve to this measurement, allowing for minimum error on the calculated total dose. The MIT-measured fast neutron dose in air in July of 2000 was 1.71 ± 0.29 cGy/min [1].

b. BNL measurement errors

In the same BNL beam, BNL researchers performed similar measurements. Bare gold foils were used to measure the thermal neutron flux in the beam. These activated gold foils were then measured with a NaI(T1) well-type detector [2]. It is important to note that the thermal neutron flux measurements cannot be directly compared between the two institutions. This is because the MIT group makes the assumption that thermal neutron activation of the Au foils is due solely to neutrons with a velocity of 2200 m/s (which have an absorption cross section of 98.8 barns [1]), while BNL calculates the energy distribution for thermal neutrons at each depth in-phantom, and then determines an associated average absorption cross section at each position. The values used by BNL for thermal neutron absorption cross section are 80.0, 83.0, and 86.0 barns at 3.5, 7.0, and 10.5 cm, respectively [1]. Since calculation of the ^{14}N and ^{10}B thermal neutron doses take these kerma factors into consideration, the thermal neutron dose calculated from the measured flux values at MIT and BNL must be compared instead. The gamma dose rates in the cube were measured using LiF-700 TLD rods, the measurements from which can be seen in Table 7. Since no measurements were made by MIT using the 8-cm collimator, these numbers cannot be used for a comparison. Again, the most accurate fast neutron dose will be obtained by scaling the RTPE output to the in-air fast neutron measurements. The BNL-measured fast neutron dose in air with the 12-cm collimator was 2.33 ± 0.35 cGy/min [2].

Since no measurements were performed by BNL in the ellipsoidal head phantom, only the Lucite cube will be used for the rest of this error analysis and dose comparison between the two institutions.

c. Physical dose comparison

From these data, the total physical dose in the Lucite cube can be calculated at specific depths in the cube by:

$$\text{Total Physical Dose} = G + N + B + F \qquad \text{[cGy/min]} \qquad \text{(Eq. 3)}$$

Where,

G = gamma dose (cGy/min)

N = ^{14}N dose (cGy/min)

B = ^{10}B dose (cGy/min)

F = fast neutron dose (cGy/min)

And, assuming the uncertainties on these measurements are independent, the absolute error on this calculated physical dose could be determined from the equation

$$\varepsilon_D = \sqrt{\varepsilon_G^2 + \varepsilon_N^2 + \varepsilon_B^2 + \varepsilon_F^2} \qquad \text{(Eq. 4)}$$

Where,

ε_G = error on the measured gamma dose

ε_N = error on the measured thermal neutron dose

ε_B = error on the measured boron dose

ε_F = error on the measured fast neutron dose

Using these equations, the values for total physical dose at 3.5, 7.0, and 10.5 cm and their associated errors can be seen in Table 9.

Table 9: Calculated physical dose rates in the Lucite cube from published MIT and BNL measurements. Errors represent the quadrature for summation. The calculations were performed with either 10 or 10 μg/g ^{10}B

Depth (cm)	MIT Physical Dose (^{10}B = 10μg/g) (cGy/min)	BNL Physical Dose (^{10}B = 10 μg/g) (cGy/min)	MIT Physical Dose (^{10}B = 20 μg/g) (cGy/min)	BNL Physical Dose (^{10}B = 20 μg/g) (cGy/min)
3.5	14.57 ± 0.75	16.45 ± 0.84	21.70 ± 1.19	24.72 ± 1.23
7.0	6.87 ± 0.39	7.66 ± 0.45	9.41 ± 0.51	10.62 ± 0.55
10.5	2.68 ± 0.18	2.83 ± 0.18	3.27 ± 0.19	2.55 ± 0.19

d. Weighted Dose Comparison

The equation to calculate weighted dose is

$$\text{Total Weighted Dose} = R_G G + R_N N + R_B B + R_F F \qquad \text{[cGy-Eq/min]} \quad \text{(Eq. 5)}$$

Where all notation is the same as above and

R_G = RBE factor for gamma dose = 1.0

R_N = RBE factor for ^{14}N thermal neutron dose = 3.2

R_B = CBE factor for ^{10}B thermal neutron dose = 1.3

R_F = RBE factor for fast neutron dose = 3.2

It is interesting to note that during the MIT clinical trials, a value of 0.5, instead of 1.0, was used for the RBE factor for gamma dose [5]. This was done because the dose in the M-67 beam was delivered slowly and was fractionated (it was delivered over two days). When calculating weighted doses, the question arises as to what error should be associated with the RBE factors. These RBE and CBE factors have all been determined experimentally [5], and unfortunately, the uncertainty on these numbers is unknown (and possibly somewhat large). This problem will be addressed first by determining the error on the weighted total dose assuming there is no error in the RBE factors, and secondly by assuming the error on the RBE factors to be as large as 20%. While the errors on the RBE factors have not been evaluated in great detail, it is known that they could possibly be quite large. A value of 20% was assumed to be a reasonable, conservative estimate of the RBE error. With no error on the RBE factors, the total dose error can be calculated by

$$\varepsilon_{DW} = \sqrt{(R_G^2\varepsilon_G^2)+(R_N^2\varepsilon_N^2)+(R_B^2\varepsilon_B^2)+(R_F^2\varepsilon_F^2)} \qquad \text{(Eq. 6)}$$

Where all notation is the same as that used previously. From this information, we get values for the weighted total dose (Gy-Eq) and its associated errors at each depth in Table 10.

Table 10: Calculated weighted dose rates from MIT and BNL measurements in the Lucite cube with either 10μg/g or 20μg/g ^{10}B, with no error on the RBE factors

Depth (cm)	MIT Weighted Dose (boron = 10 μg/g) (cGy-Eq/min)	BNL Weighted Dose (boron = 10 μg/g) (cGy-Eq/min)	MIT Weighted Dose (boron = 20 μg/g) (cGy-Eq/min)	BNL Weighted Dose (boron = 20 μg/g) (cGy-Eq/min)
3.5	20.38 ± 0.95	22.77 ± 1.00	29.66 ± 1.53	33.51 ± 1.54
7.0	8.92 ± 0.44	9.91 ± 0.49	12.22 ± 0.61	13.76 ± 0.63
10.5	4.63 ± 0.41	4.68 ± 0.41	5.39 ± 0.42	5.79 ± 0.42

If a 20% error on the RBE factors is now assumed, the error equation becomes

$$\varepsilon = \sqrt{(G^2)(R_G^2)((\frac{\varepsilon_G}{G})^2+(0.2^2))+(N^2)(R_N^2)((\frac{\varepsilon_N}{N})^2+(0.2^2))+(B^2)(R_B^2)((\frac{\varepsilon_B}{B})^2+(0.2^2))+(F^2)(R_F^2)((\frac{\varepsilon_F}{F})^2+(0.2^2))} \quad \text{(Eq. 7)}$$

The weighted total doses and their associated errors at each depth calculated from this equation can be seen in Table 11.

Table 11: Calculated weighted dose rates from MIT and BNL measurements in the Lucite cube with either 10μg/g or 20μg/g ^{10}B with 20% error on the RBE factors

Depth (cm)	MIT Weighted Dose (boron = 10 μg/g) (cGy-Eq/min)	BNL Weighted Dose (boron = 10 μg/g) (cGy-Eq/min)	MIT Weighted Dose (boron = 20 μg/g) (cGy-Eq/min)	BNL Weighted Dose (boron = 20 μg/g) (cGy-Eq/min)
3.5	20.38 ± 2.51	22.77 ± 2.83	29.66 ± 4.25	33.51 ± 4.82
7.0	8.92 ± 1.13	9.91 ± 1.26	12.22 ± 1.66	13.76 ± 1.88
10.5	4.63 ± 0.69	4.86 ± 0.70	5.39 ± 0.74	5.79 ± 0.77

2. Phantom Evaluation

To begin a comparison of the patient doses at BNL and MIT, the Lucite cube is used to determine scaling factors between measurements made by the two institutions. Measurements were taken at the BNL beam with the 12-cm collimator by MIT researchers in June and September of 2000, and are summarized in Table 6 [1]. Measurements by BNL researchers were also taken in the same beam with both the 8-cm collimator and the 12-cm collimator in place, and are summarized in Table 7 [2]. Systematic differences in measured values between BNL and MIT groups in the same beam have been documented [1]. To compare and combine patient data from both MIT and BNL clinical trials, it is necessary to analyze these dosimetry measurement differences and apply a "correction factor" to one set. In this thesis, the BNL patient dosimetry data will be adjusted to agree with MIT measurements.

Since the prescribed patient doses were generated from RTPE, and these are the numbers that ultimately need to be evaluated, the RTPE output, not the BNL measurements, should be compared against the MIT measurements for the sake of consistency. Since the RTPE source definition models the BMRR epithermal neutron beam very closely, the BNL measurements and the RTPE output should match up very well. This can be checked for gamma dose and thermal neutron flux. Figure 11 and Figure 12 show the thermal neutron flux and gamma dose rate measurements,

respectively, compared to the RTPE output. These graphs show that the BNL measurements do in fact match up well with the RTPE output, particularly the thermal neutron flux, which has the greatest effect on the total dose. Therefore, it is valid to compare the RTPE output to the MIT measurements.

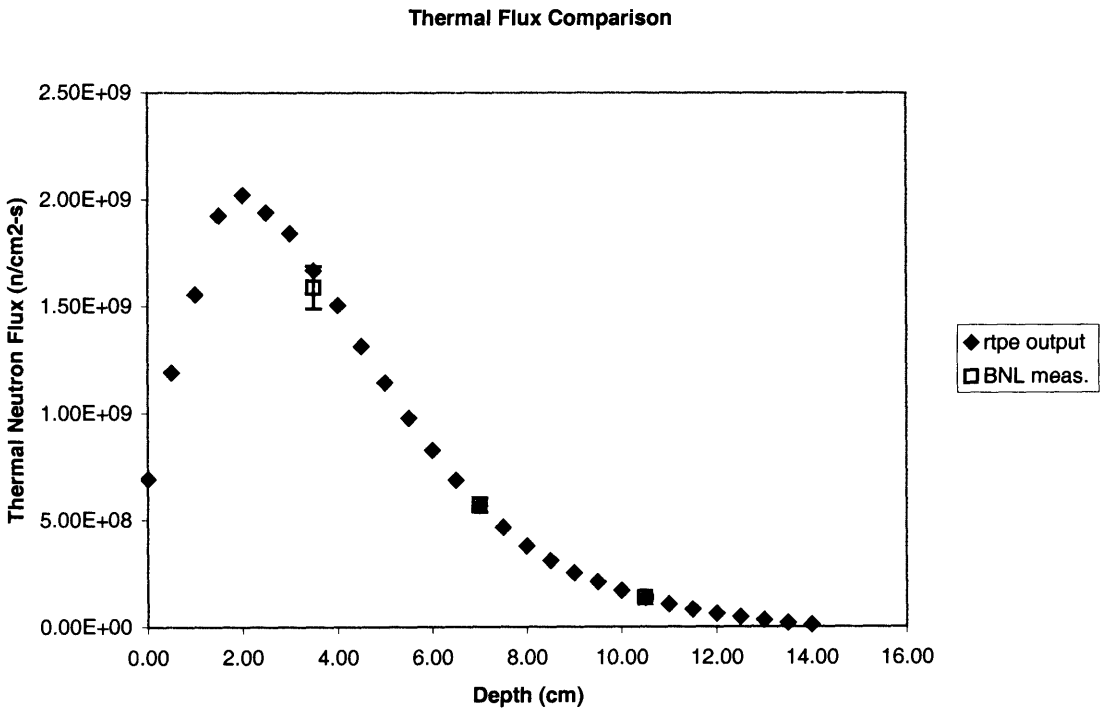

Figure 11: BNL thermal neutron flux measurements [2] compared to RTPE output in the Lucite cube with the 12-cm collimator

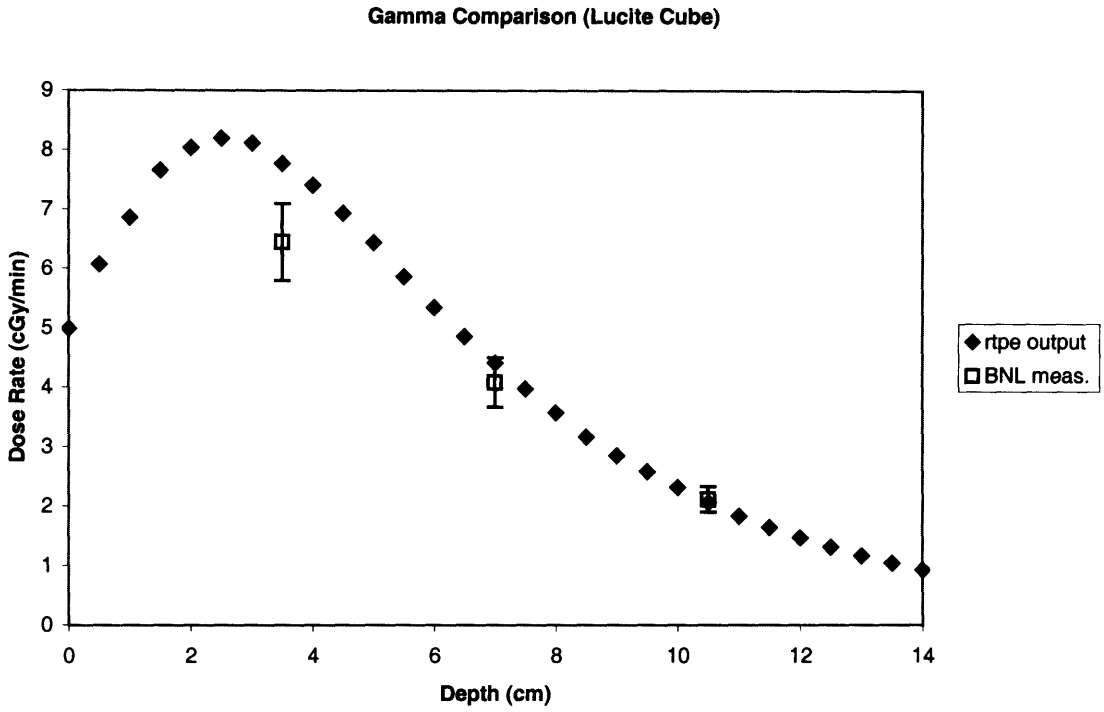

Figure 12: BNL gamma dose rate measurements [2] compared to the RTPE gamma dose rate output in the Lucite cube for the 12-cm collimator

Since the approach taken for this combination of patient data is to adjust the BNL patient doses to match the MIT measurements of the BMRR epithermal neutron beam, it is necessary to examine each dose component individually and to compare the depth-dose curves in the Lucite cube for both the MIT measurements with the RTPE output. Once scaling factors have been determined in the Lucite cube, they can be applied to the ellipsoidal head phantom. Using this additional phantom will provide a check on the scaling factors calculated from the Lucite cube. It is expected that with the use of the scaling factors, the output from the ellipsoidal head phantom will match up well with the measurements performed in the BMRR epithermal neutron beam by MIT in the same phantom.

3. Thermal Neutron Dose

As mentioned above, the thermal neutron flux was measured by MIT, and thus the thermal neutron doses due to ^{14}N and ^{10}B can be calculated using Equations 1 and 2.

Different cross sections were used for thermal neutrons by MIT and BNL, so the fluxes cannot be directly compared. Because of this, it is important that the thermal doses (^{14}N and ^{10}B) instead be calculated and compared. In determining the scaling factors, the simple ratio of MIT dose divided by the BNL dose at the same depth is calculated. When this is done, a scaling factor can be calculated that scales the RTPE thermal neutron dose output to match the MIT measurements using a least squares fit. The fractional error on the scaling factor is equal to the fractional error for each of the MIT measurements. The scaling factor calculated in the Lucite cube for this dose component is 0.90±0.07. Because both the ^{14}N and ^{10}B dose components are calculated from the thermal neutron flux, both should have a similar scaling factor between the BNL doses and the MIT measurements. When calculated, the scaling factor for the ^{10}B component in the Lucite cube was 0.93±0.07. As it is clearly seen, the two are in fact very close, and the error bars overlap. Therefore, one scaling factor for both thermal neutron dose components will be calculated by averaging the two individual scaling factors, and a thermal neutron scaling factor of 0.92±0.07 will be used. Figure 13 and Figure 14 show the ^{14}N dose and the ^{10}B dose in the Lucite cube with and without this adjustment factor of 0.92.

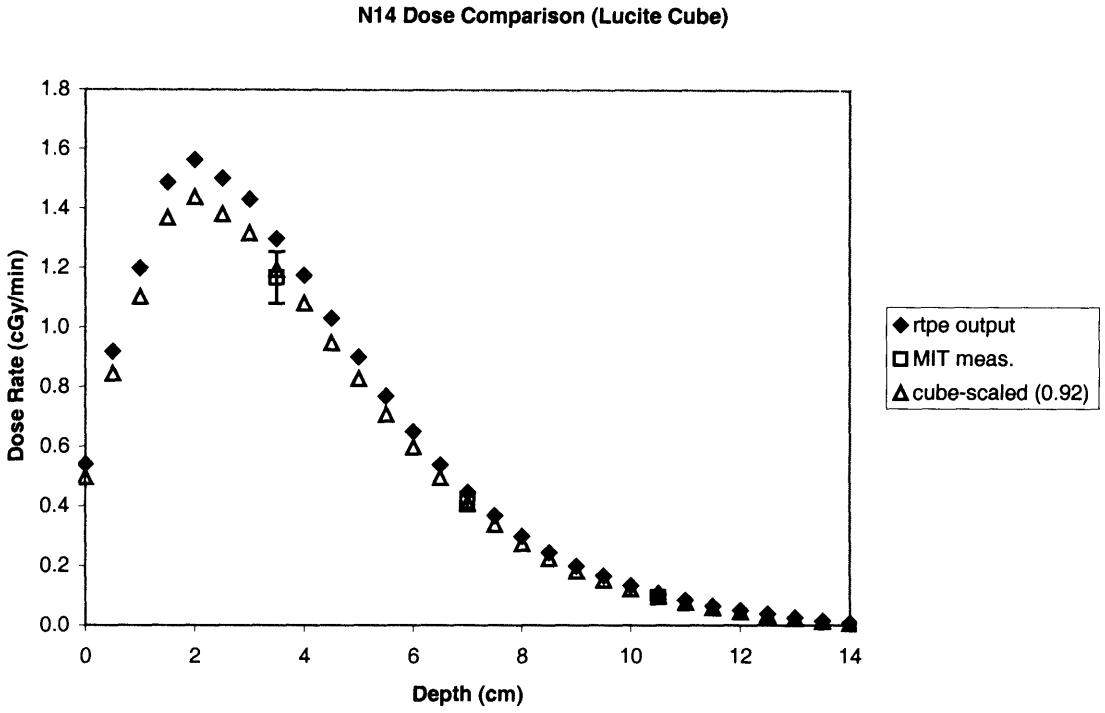

Figure 13: ^{14}N dose rate scaling in Lucite cube with scaling factor 0.92 compared to original RTPE ^{14}N dose rate output and ^{14}N dose rates calculated from MIT measurements

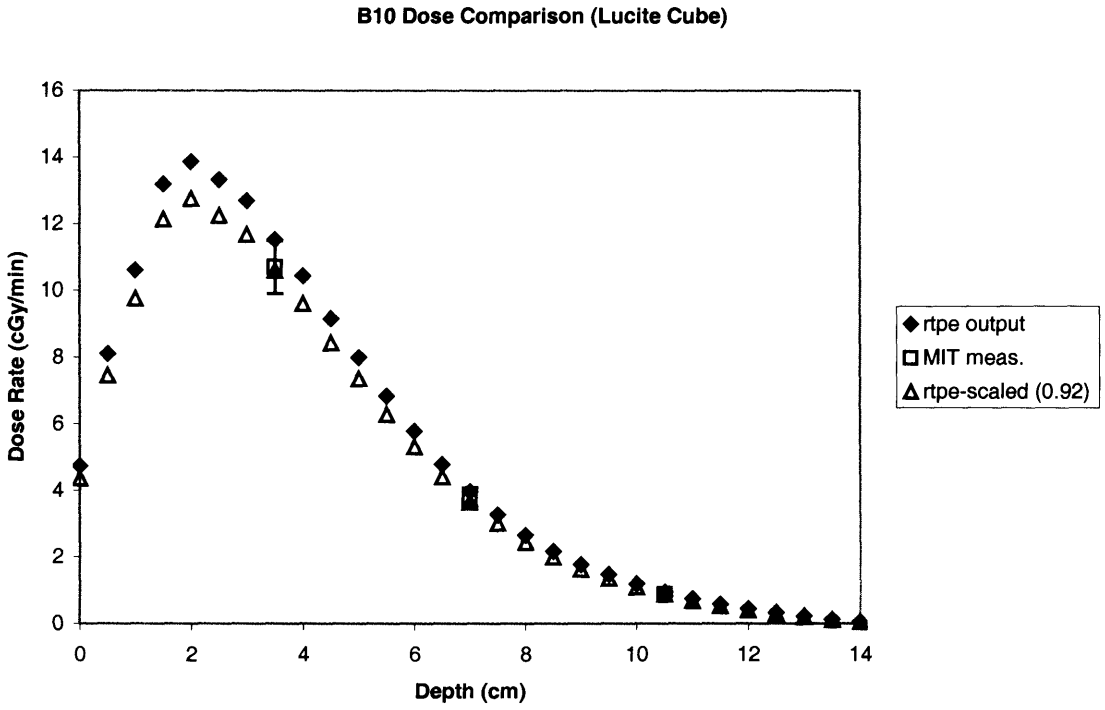

Figure 14: ^{10}B dose scaling in Lucite cube with 15ppm ^{10}B with scaling factor 0.92 compared to original RTPE ^{10}B dose rate output and ^{10}B dose rates calculated from MIT measurements

4. Gamma Dose

The same sort of comparison is performed on the gamma dose rates. When the least squares fitting is applied to the Lucite cube RTPE gamma dose rate output, a scaling factor of 0.74±0.06 is calculated by dividing the MIT measurement by the BNL measurement at each depth that a measurement was performed. The output from RTPE with and without this scaling factor can be seen in Figure 15.

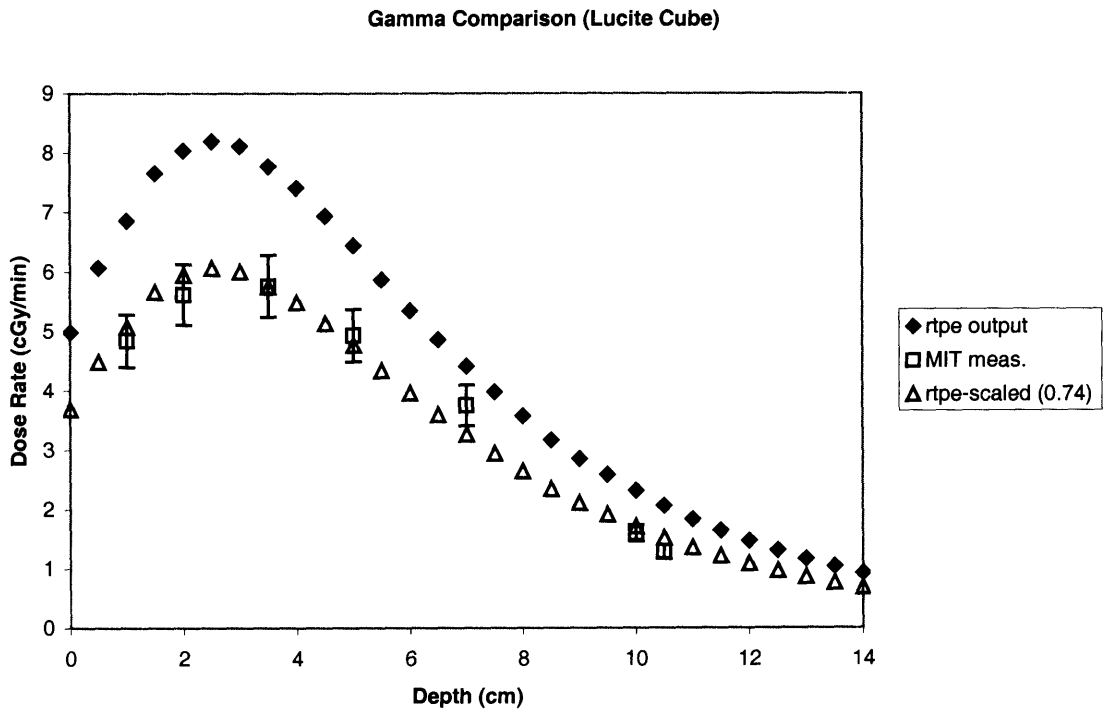

Figure 15: Photon dose rate in the Lucite cube with a scaling factor of 0.74 compared to original unscaled RTPE photon dose rate output and MIT photon dose rate measurements

5. Fast Neutron Dose

As mentioned previously, the error on the fast neutron measurements in the phantoms is quite large due to the greater subtraction for photons in-phantom. Since the error on the in-air measurements is much smaller, these measurements will be used to obtain the fast neutron scaling factor. The MIT in-air fast neutron measurement was 1.71±0.29 cGy/min [1], and the BNL in-air fast neutron measurement was 2.33±0.35 cGy/min [1]. The scaling factor obtained from these measurements is 0.73±0.12. To obtain this scaling

factor, the MIT in-air measurement was divided by the BNL in-air measurement, and the fractional error on the scaling factor is the same as the greater fractional error on the two measurements (17%). Figure 16 shows the Lucite phantom fast neutron dose output, both scaled and unscaled, compared to the in-air fast neutron measurements by MIT and BNL.

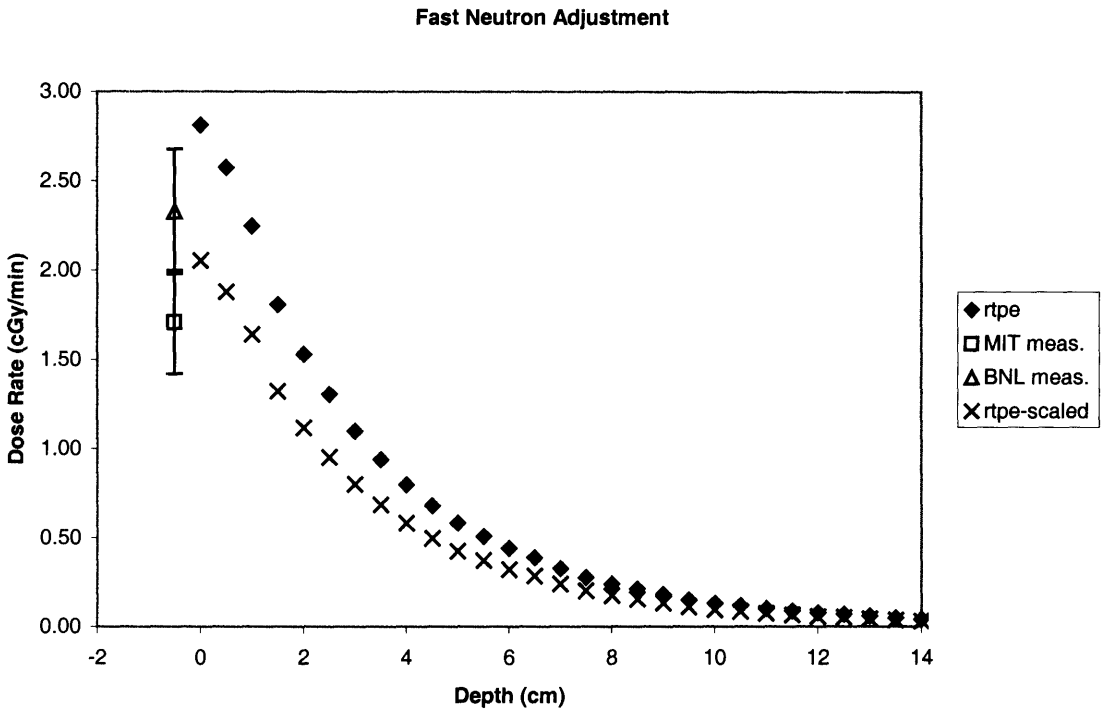

Figure 16: In-air fast neutron measurements by both BNL and MIT compared to fast neutron RTPE output in Lucite cube phantom with a scaling factor of 0.73 and original, unscaled RTPE output

6. Ellipsoidal Head Phantom

To check these scaling factors, the ellipsoidal head phantom can be used. Since measurements were performed in the BMRR epithermal neutron beam by MIT in this phantom, running the head phantom through RTPE with the scaling factors applied should yield dose curves that match with the MIT measurements. The curves for each of the dose components can be seen in Figure 17, Figure 18, Figure 19, and Figure 20. These graphs show that the results from the head phantom do, in fact, match up fairly well with the MIT measurements, especially when the error on the scaled RTPE curve is taken into consideration. The error on the scaled RTPE curve arises mainly from the

error on the scaling factors, but partially from the error inherent with RTPE. This error comes to between about 5% and 10%, and will cause the scaled RTPE curve to overlap with the MIT measurements.

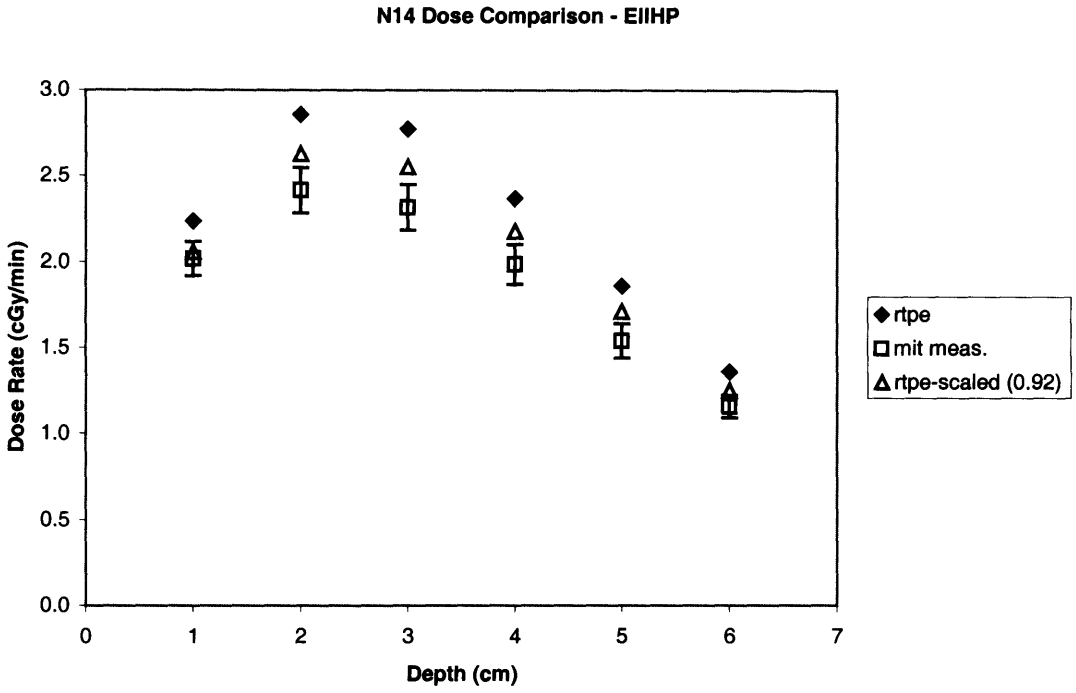

Figure 17: Unscaled RTPE ^{14}N doses in the ellipsoidal head phantom, ^{14}N doses calculated from MIT measurements, and the scaled RTPE output using a scaling factor of 0.92

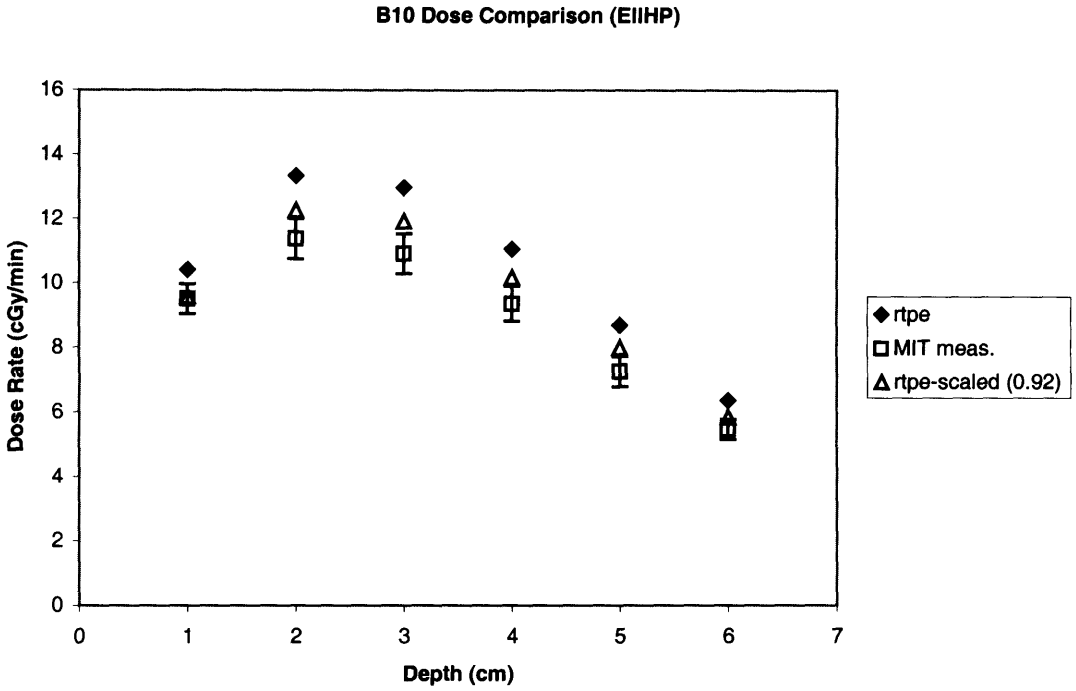

Figure 18: Unscaled RTPE ^{10}B doses in the ellipsoidal head phantom, ^{10}B doses calculated from MIT measurements, and the scaled RTPE output using a scaling factor of 0.92

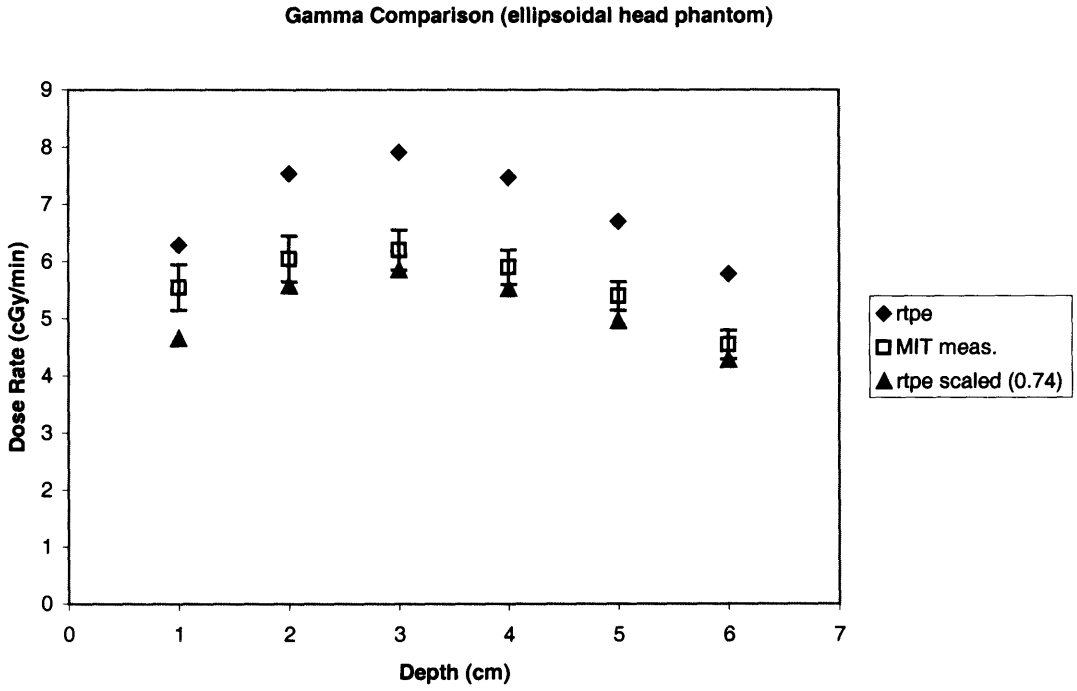

Figure 19: Unscaled RTPE gamma doses in the ellipsoidal head phantom, gamma doses measured by MIT, and the scaled RTPE output using a scaling factor of 0.74

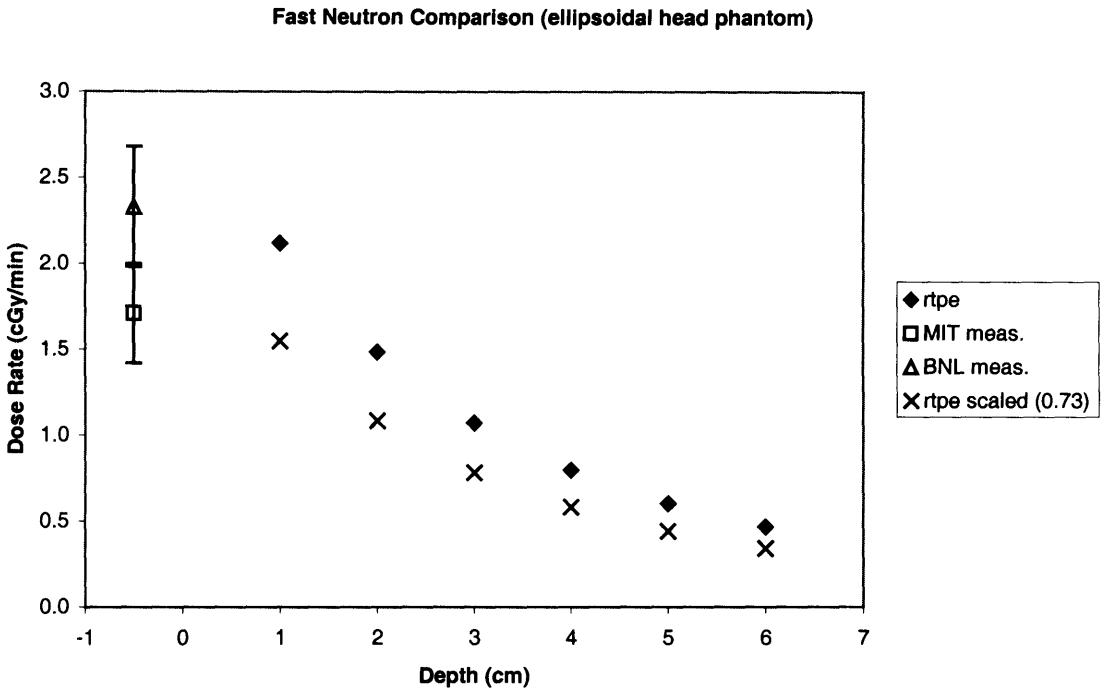

Figure 20: Unscaled RTPE fast neutron doses in the ellipsoidal head phantom, in air fast neutron doses measured by MIT and BNL, and the scaled RTPE output using a scaling factor of 0.73

7. Total Physical Dose

The final adjustment factors are summarized in Table 12.

Table 12: Adjustment factors necessary to scale RTPE output to match MIT measurements

	^{14}N	^{10}B	Gamma	Fast Neutron
Scaling Factor:	0.92	0.92	0.74	0.73

Now that the individual adjustment factors have been determined, it is necessary to see how these factors must be combined to ultimately adjust the BNL patient brain doses (both peak and whole brain average). By applying all the factors together, we determine:

$$D = 0.74D_G + 0.92D_N + 0.92D_B + 0.73D_F \quad \text{in cGy/min} \quad \text{(Eq. 8)}$$

Where D_G is the gamma component of the total dose, D_N is the ^{14}N thermal neutron component of the total dose, D_B is the boron component of the total dose, and D_F is the fast neutron component of the total dose. The top curve in Figure 21 shows the original RTPE output in the Lucite cube, along with this new lower adjusted total dose in the Lucite cube and the MIT total physical dose calculated from the MIT measurements.

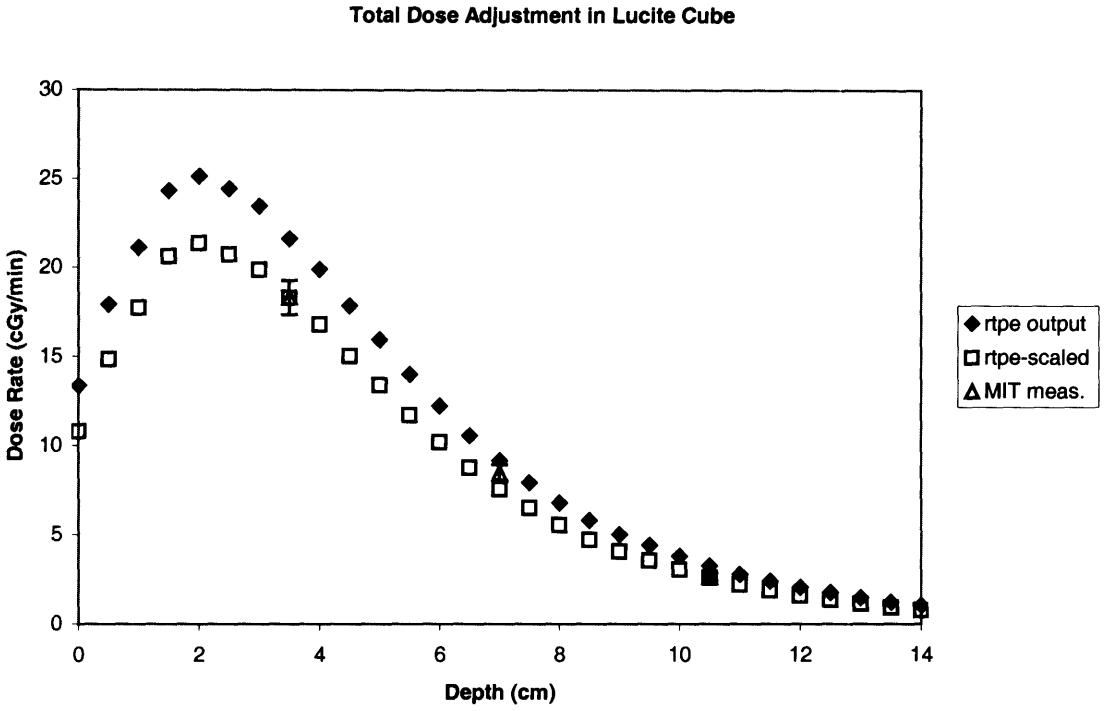

Figure 21: Total physical dose rate output from RTPE with and without adjustment factors in Lucite cube with 15ppm ^{10}B compared to total physical dose calculated from MIT measurements

The difference between the two physical dose rate curves ranges from 15% to 25% depending on depth in the cube. At the peak, the adjusted curve is 15% lower than the original curve for the Lucite cube. On average the adjusted curve is about 18% lower than the original curve in the cube.

Further analysis of this curve (i.e., finding a more accurate, single adjustment factor for the total dose curve) will not be done because this adjustment factor would only apply to two-dimensional analyses. Since we are more interested in the effect on patient dose-volume histograms and peak and whole brain average doses, further work with the phantoms is unnecessary.

8. Weighted Doses

Prescribed patient doses are quoted in terms of weighted doses (Gy-Eq), so it is important to observe the effect of the adjustment factors on weighted doses in the phantoms. The weighted doses can be obtained by applying the RBE factors mentioned

previously. When the adjustment factors are applied to the Lucite cube and compared to the weighted doses calculated from the MIT measurements, Figure 22 is obtained. These calculated MIT doses assumes no error in the RBE factors. Figure 23 shows the total weighted dose calculated assuming a 20% error on the RBE factors.

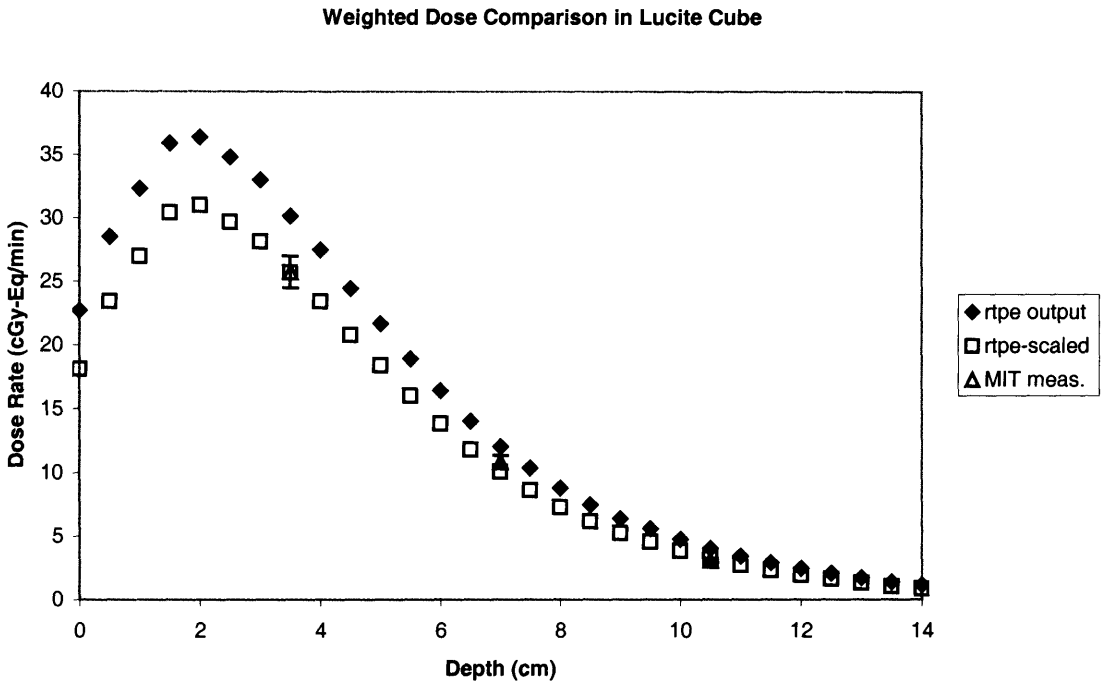

Figure 22: Adjusted and unadjusted total weighted dose in Lucite cube with 15ppm ^{10}B from RTPE compared to total weighted dose calculated from MIT measurements

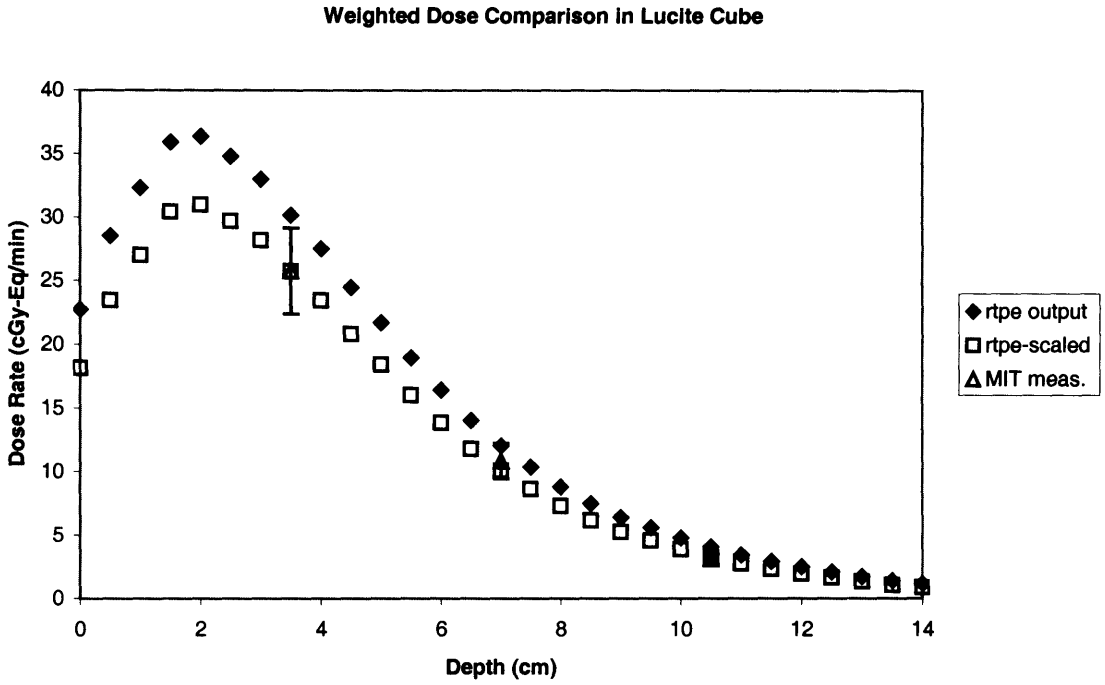

Figure 23: Adjusted and unadjusted total weighted dose rates in the Lucite cube with 15ppm ^{10}B from RTPE compared to total weighted dose calculated from MIT measurements assuming 20% error on RBE factors

References:

1. K.J. Riley, P.J. Binns, D.D. Greenberg, O.K. Harling, A physical dosimetry intercomparison for BNCT, Med. Phys., **29:** 898-904 (2002).

2. H.B. Liu, D.D. Greenberg, J. Capala, An improved neutron collimator for brain tumor irradiations in clinical boron neutron capture therapy, Medical Physics, **23:** pages (1996).

3. D. Greenberg, unpublished data

4. Saraf, S. K., J. Kalef-Ezra, R. G. Fairchild, B. H. Laster, S. Fiarman, and E. Ramsey, Epithermal beam development at the BMRR: Dosimetric evaluation: In Neutron Beam Design, Development, and Performance for Neutron Capture Therapy (O. K. Harling, Ed.), pp. 307–316. Plenum Press, New York, 1990.

5. J.A. Coderre, G.M. Morris, The Radiation Biology of Boron Neutron Capture Therapy, Radiation Research, **151:** 1-18 (1999).

6. K.J. Riley, P.J. Binns, O.K. Harling, Performance characteristics of the MIT fission converter based epithermal neutron beam, Physics in Medicine & Biology, **48:** 943-958 (2003).

V. Application of Scaling Factors

1. Applying Adjustment to Patient Data

Now that the comparison of the beam components is complete, the values determined to be the necessary adjustment factors can be applied to the BNL patient data. All the patients have a different ^{10}B concentration, and the adjustment must be applied to a three-dimensional output, and therefore a single adjustment factor cannot be applied to the existing defined peak and whole-brain average doses. To apply the adjustment, the patient treatment plans were rerun in RTPE, with the adjustment factors included in the input file. The actual particles need not be rerun; only the dose calculation edits need to be rerun. Therefore, changes were made to the definitions of the RBE factors in the edit directives section of the input file. By multiplying the existing RBE factors by the new scaling factors corresponding to the same dose component, both the RBE factors and the adjustment factors can be applied to this dose component. Table 13 shows the new peak and average brain doses obtained when all of the BNL patients are rerun in RTPE. As can be seen, the new peak dose numbers are about 16% lower than the original numbers. The new whole-brain average doses are about 18% lower than the original RTPE output.

It is of particular interest to observe the effect the adjustment factors have on the dose distribution in normal brain tissue. This can be viewed by looking at the integral dose-volume histogram (DVH) information RTPE outputs. Figure 24, Figure 25, and Figure 26 show representative DVHs for 1, 2, and 3-field patient treatment plans, respectively. The solid line in each figure represents the original DVH, and the dotted line represents the DVH of the treatment plans rerun with the adjustment factors. These plots show that the general shape of the curve remains the same, but the curves are simply shifted. Therefore, the fractional dose distribution in the normal brain tissue does not change significantly when the BNL dose is adjusted to match the MIT dose, even though the peak dose changes by about 16%. Table 13 shows all BNL patients from protocols 1-8 with and without the adjustment factors applied to their peak and whole-brain average dose values.

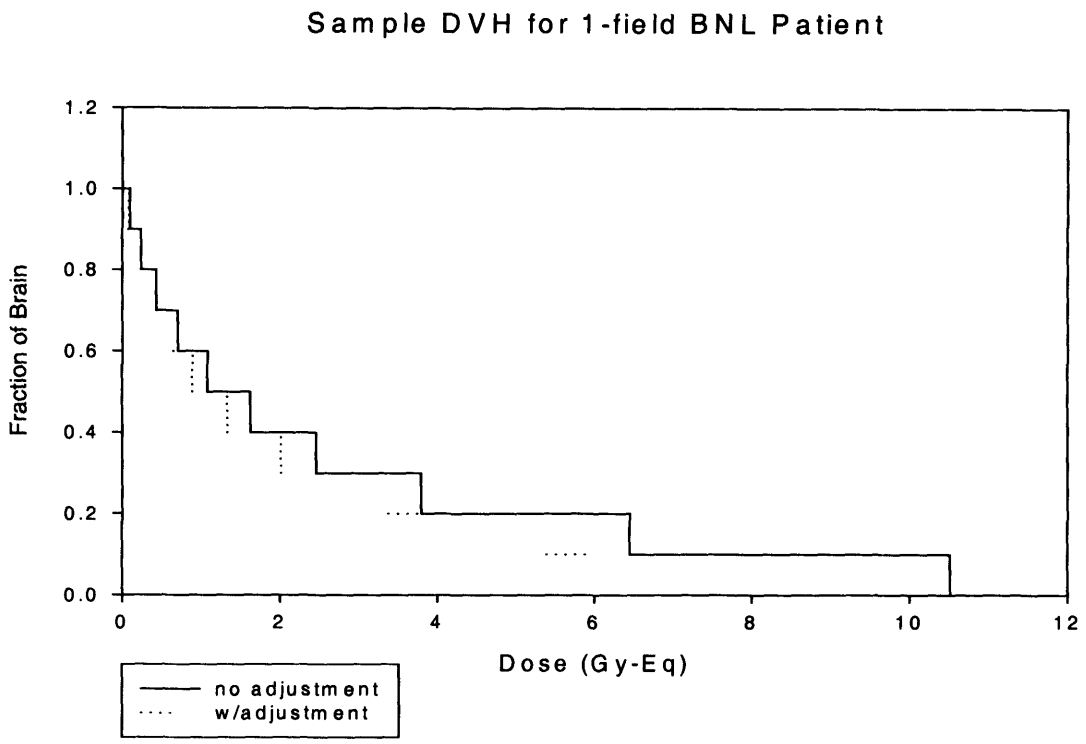

Figure 24: Dose volume histogram for 1-field BNL treatment plan with and without adjustment factors

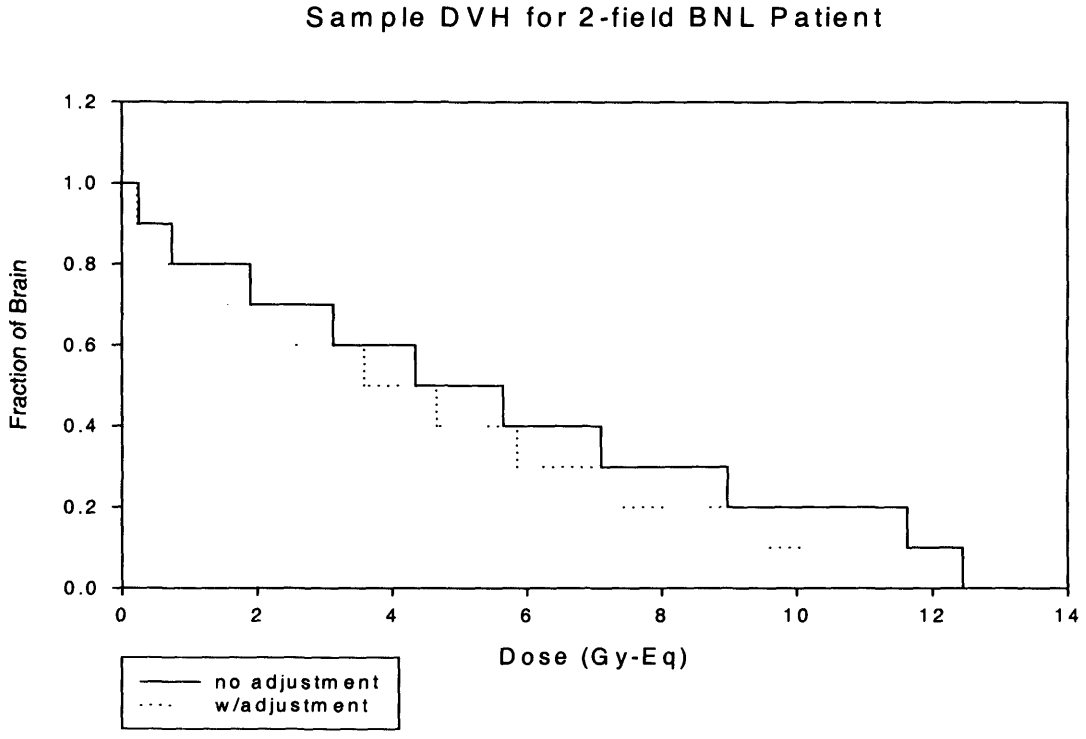

Figure 25: Dose volume histogram for 2-field BNL treatment plan with and without adjustment factors

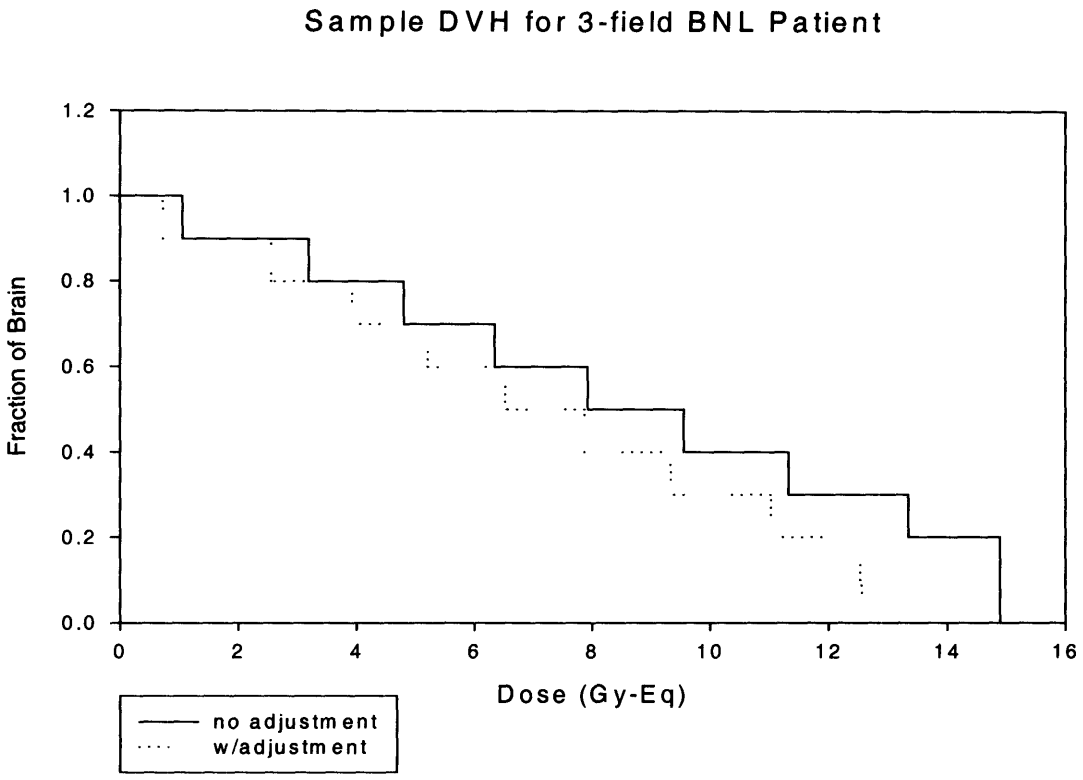

Figure 26: Dose volume histogram for 3-field BNL treatment plan with and without adjustment factors

Table 13: BNL data on patients treated with BNCT – date of treatment, number of fields each patient was treated with, and unadjusted and adjusted peak and whole brain average weighted doses

Pt #	Date	# of fields	Original Peak (Gy-Eq)	Adjusted Peak (Gy-Eq)	Original Average (Gy-Eq)	Adjusted Average (Gy-Eq)
1	9/13/94	1	10.08	8.40	2.31	1.87
2	2/2/95	1	8.88	7.45	2.04	1.67
3	4/13/95	1	10.52	8.79	2.13	1.74
4	4/27/95	1	10.53	8.79	2.23	1.81
5	6/15/95	1	10.86	9.06	1.93	1.57
6	6/22/95	1	10.51	8.83	2.24	1.84
7	6/29/95	1	10.28	8.58	2.27	1.85
8	6/30/95	1	13.26	11.01	2.66	2.16
9	7/13/95	1	10.97	9.22	2.85	2.34
10	7/20/95	1	10.67	9.01	2.09	1.72
11	10/5/95	1	10.80	9.07	2.27	1.86
12	10/13/95	1	11.63	9.65	2.23	1.80
13	11/30/95	1	10.62	8.88	2.64	2.15
14	2/1/96	1	12.65	10.52	2.44	1.98
15	2/22/96	1	13.14	10.95	2.40	1.94
16	6/6/96	2	11.94	10.06	4.55	4.14
17	6/13/96	1	12.60	10.70	3.35	2.87
18	7/11/96	2	12.95	10.72	4.93	4.00
19	7/25/96	2	12.86	10.63	4.50	3.72
20	8/1/96	2	13.75	11.42	5.72	4.67
21	9/12/96	1	14.22	11.85	4.16	3.38
22	9/19/96	1	13.16	11.01	3.72	3.02
23	10/17/96	1	14.39	12.08	3.74	3.13
24	11/7/96	1	12.45	11.03	3.41	2.80
25	11/14/96	1	12.27	10.22	3.26	2.65
26	12/11/96	1	12.61	10.57	3.76	3.08
27	12/18/96	2	11.90	9.83	5.24	4.22
28	1/9/97	2	12.19	10.07	4.08	3.38
29	1/23/97	2	11.94	10.07	4.84	3.93
30	1/30/97	1	12.48	10.73	3.70	3.12
31	5/29/97	1	13.80	11.56	3.59	2.93
32	6/11/97	1	13.05	10.90	3.73	3.03
33	6/18/97	2	12.60	10.58	5.30	4.35
34	8/13/97	2	12.45	10.45	5.00	4.12
35	10/8/97	2	12.78	10.77	5.27	4.39
36	11/12/97	1	14.83	12.66	3.79	3.23
37	12/31/97	2	13.34	11.22	5.95	4.89
38	2/4/98	2	12.57	10.59	4.69	3.86
39	6/3/98	2	12.73	10.67	5.46	4.46
40	6/24/98	2	12.21	10.16	6.57	5.35
41	8/19/98	2	12.40	10.50	5.31	4.49
42	10/21/98	3	14.59	12.03	9.38	7.60
43	11/25/98	3	14.91	12.55	7.99	6.60
44	12/2/98	3	15.63	13.26	8.36	6.97

45	12/9/98	2	12.92	10.94	5.22	4.32
46	12/10/98	3	14.65	12.38	8.09	6.70
47	12/16/98	3	15.43	12.88	8.13	6.65
48	12/17/98	2	11.29	9.54	4.78	3.95
49	1/13/99	3	15.64	13.05	9.07	7.41
50	3/10/99	3	14.13	11.99	8.70	7.21
51	3/26/99	3	14.77	12.40	6.71	5.50
52	4/28/99	3	9.5	7.97	4.4	3.60
53	5/7/99	3	12.6	10.58	7.6	6.24
54	5/20/99	3	14.0	11.77	7.5	6.15

2. Applying Adjustment to Tumor Data

Another important application of these scaling factors is to tumor doses. It is important to know what dose the tumors are getting because it is these cells that the treatment is targeting. If the tumor cells do not get sufficient dose, they will not die, and the tumor will recur following treatment. Unfortunately, since the limiting factor in how much dose can be administered during BNCT is normal tissue tolerance, the tumors frequently do not get enough dose and do in fact recur. However, it will be interesting to pool tumor doses along with the whole brain doses. Table 14 shows the doses applied to BNL patients' tumors before and after the scaling factors have been applied. It is important to note that researchers are more uncertain of the ^{10}B CBE factor in tumor. The CBE factor used for BPA is 3.8 [2]. Ideally, CBE factors for BPA and BSH should be derived using survival data, but this has been difficult with the intracranial 9L gliosarcoma due to the normal tissue complications resulting from the large single fractions of X rays needed to control this tumor [2]. Additionally, it is not known whether or not all tumor cells accumulate boron. Figure 27 shows a sample tumor DVH for a 1-field patient with and without the adjustment factors.

Table 14: Adjusted and unadjusted peak and average weighted doses to tumor for each patient treated with BNCT at BNL

Pt #	Original Peak (Gy-Eq)	Adjusted Peak (Gy-Eq)	Original Average (Gy-Eq)	Adjusted Average (Gy-Eq)	Pt #	Original Peak (Gy-Eq)	Adjusted Peak (Gy-Eq)	Original Average (Gy-Eq)	Adjusted Average (Gy-Eq)
1	47.60	41.39	42.37	38.35	28	56.00	50.74	52.00	47.26
2	53.79	40.02	45.45	40.61	29	66.00	52.86	55.00	50.25
3	49.46	45.09	41.89	38.35	30	58.00	53.48	50.00	45.73
4	48.69	43.91	37.67	33.67	31	66.00	59.91	57.00	51.64
5	50.53	46.00	37.55	33.83	32	59.00	54.06	55.00	50.38
6	47.52	48.22	40.48	41.95	33	68.00	61.88	65.00	59.15
7	48.60	43.41	37.30	33.32	34	65.00	59.97	55.00	50.21
8	64.36	53.92	48.10	42.27	35	65.00	59.03	52.00	47.65
9	54.50	49.66	43.45	40.23	36	83.70	76.69	74.90	68.65
10	55.57	50.77	46.23	42.02	38	63.83	58.40	63.31	57.83
11	51.52	48.64	48.29	45.06	39	59.23	53.86	46.35	42.05
12	53.82	46.53	37.33	33.24	41	66.11	60.45	56.69	51.91
13	50.73	44.87	44.08	40.92	45	69.37	63.45	39.04	35.54
14	56.37	51.18	42.43	38.35	48	59.09	53.99	55.14	50.27
15	60.67	55.15	38.52	35.00	37	65.99	58.62	54.61	49.98
16	60.00	63.78	49.36	51.98	40	53.00	48.13	47.00	42.52
17	63.00	57.88	53.00	48.16	42	60.19	54.45	54.11	48.80
18	56.00	50.46	37.00	30.75	43	76.84	70.14	64.40	58.66
19	54.00	49.20	45.00	39.53	44	86.31	78.54	79.19	72.40
20	58.00	56.22	47.00	45.65	46	78.57	71.83	69.73	63.72
21	62.00	57.94	48.00	44.18	47	72.28	65.77	53.80	48.81
22	61.00	52.22	48.00	43.50	49	73.20	66.59	64.96	58.94
23	69.00	62.78	59.00	53.42	50	77.93	71.33	63.16	57.68
24	68.00	62.15	58.00	53.09	51	77.72	70.73	63.08	57.40
25	55.00	50.21	51.00	46.11	52	54.14	49.27	43.97	40.01
26	60.00	54.60	47.00	42.77	53	48.22	43.88	31.74	28.88
27	49.00	44.66	36.00	32.13	54	75.33	68.55	54.19	49.31

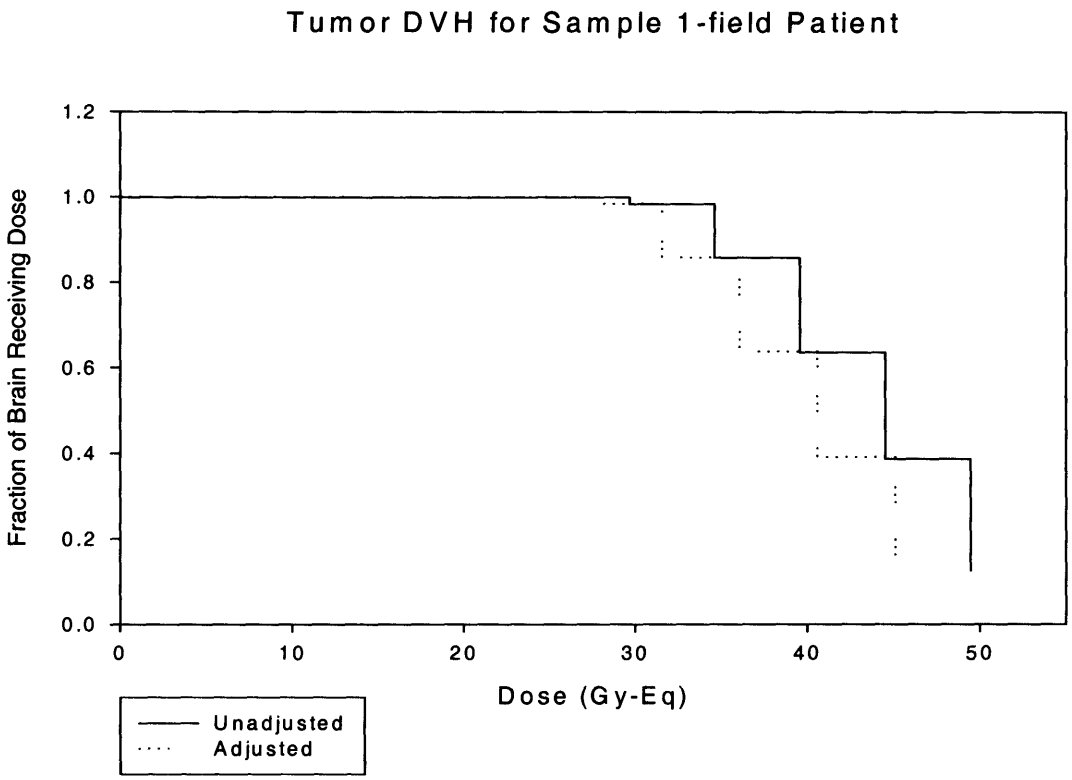

Figure 27: Dose volume histogram to tumor for sample 1-field BNL treatment plan with and without adjustment factors

References

1. J.A. Coderre, J.C. Turcotte, K.J. Riley, P.J. Binns, O.K. Harling, W.S. Kiger III. "Boron Neutron Capture Therapy: Cellular Targeting of High Linear Energy Transfer Radiation", Technology in Cancer Research & Treatment, **2:** 355-375 (2003).

2. J.A. Coderre, G.M. Morris, The Radiation Biology of Boron Neutron Capture Therapy, Radiation Research, 151: 1-18 (1999).

VI. Somnolence Endpoint

With traditional photon therapy administered to tumors in the brain, there are a number of side effects the radiation can cause. These side effects are divided into two categories: acute and delayed. Acute effects occur immediately following radiation treatment (a few days to a few weeks), and are generally temporary or can be managed with medical interventions. Acute effects in the CNS are not necessarily due to damage to the normal brain. One acute effect reported in both the BNL and the MIT BNCT clinical trials is an increase in intracranial pressure due to the response of residual tumor volumes that were larger than 60 cc [1, 2]. Delayed effects occur much later, and can be classified as either early or late. Early delayed effects typically occur between one and six months following treatment. Late delayed effects occur six months or more after therapy and are usually irreversible. One delayed side effect is necrosis, which is death of normal cells or tissue. Necrosis in normal brain tissue can lead to undesirable effects on the patient's motor skills, speech, etc, depending on the location and the volume of the area involved. Necrosis is characterized as a late delayed effect, is irreversible, and can be lethal [3]. Another delayed side effect is somnolence syndrome, which is characterized by periods of drowsiness, lethargy, loss of appetite, and irritability following radiation treatment. Somnolence is an early delayed effect. The somnolence syndrome was first observed in children treated with brain irradiation as part of a whole-body irradiation-conditioning regimen prior to bone marrow transplant, but it is also frequently observed in adults treated for brain tumors [4]. Both necrosis and somnolence have also been observed in BNCT. Necrosis has been reported in some of the long-term survivors of the Japanese BNCT protocols [5].

It has been of great interest to determine the cause of these radiation side effects. The mechanism of radiation induced side effects in the brain and other tissues is still a matter of considerable debate: the question is whether the target cell population is the vascular endothelial cells or the functional brain cells [6]. The cause has been thought to be a primary cell population, the inactivation of which, following irradiation, results in these side effects [3]. Additionally, it has been observed that the lesions in the central nervous system (CNS) following irradiation are similar to the lesions created following other types of CNS damage, and therefore the reaction of the CNS to irradiation may have

similar mechanisms to other forms of damage. Direct damage to the CNS results in acute cell death, secondary reactive processes, and enhanced cytokine gene expression [3]. These responses have all been observed following radiation injury as well.

During BNCT, as with other types of radiation therapy, the cause of the side effects is simply the administration of too high a dose, either to the whole brain or to a specific region of the brain. During the BNCT clinical trials, one of the objectives was to determine what this brain tolerance was. There are three phases of clinical trials. A phase I clinical trial is a safety and dose-escalation study. The dose administered to small groups of patients is slowly increased over time until an unsatisfactory endpoint is reached. A phase II clinical trial is performed after the phase I trial is completed, and is performed to further determine side effects and how to manage them, as well as to determine the most effective dose to use during treatment. In a phase III trial, the new treatment is compared against currently existing treatments and to determine how effective these new treatments are. Phase III trials use large enough numbers of patients for statistical significance.

During the BNCT clinical trials, the question arose as to what endpoint should be used to determine the maximum brain dose acceptable to administer to the patient. Death, or length of survival post-BNCT, is an unacceptable endpoint due to a couple of factors. One is that before a radiation dose high enough to cause death is administered, effects on the patient's mental status will be seen. Secondly, the unfortunate fact is that even with BNCT, all the patients will die, usually within a year, and it is almost impossible to know how much the BNCT contributed to that death. In other words, patients with GBM generally do not live long enough to develop the classic late effects in the brain. Additionally, a patient may receive another form of therapy following BNCT, and it is impossible to know to what extent BNCT contributed to the patient's quality of life following all of his or her treatments. The only other side effect that has been seen as a reasonable endpoint is somnolence.

In traditional radiotherapy, somnolence has been found to occur in a somewhat cyclical pattern. It has been found that somnolence occurs in patients typically between about day 11 and day 21 and from about day 31 to day 35 following radiotherapy. While the severity of the symptoms was shown to increase due to accelerated fractionation, the

cyclical pattern of the symptoms did not change [2]. It has been determined that necrosis is related to location of the irradiation and the total volume of brain tissue that receives greater than 12 Gy of photons [7]. Flickinger et. al. [8] showed that the volume of tissue receiving 12 Gy or more (termed the "12-Gy-Volume") accurately reflected the risk of postradiosurgery MRI images showing changes indicating radiation damage. It is well recognized that the occurrence of side effects are directly related to the volume of brain tissue irradiated. This most likely holds for BNCT as well as for conventional radiotherapy. In BNCT, the dose is administered as a whole-brain dose. Because of this, the occurrence of somnolence could be a combination of multiple locations receiving a dose sufficient to cause somnolence.

1. Peak and whole brain average dose relationship

54 patients were treated with BNCT at BNL during the duration of their clinical trial. Of these 54 patients, 11 showed symptoms of somnolence. These 11 included 9 patients treated with 3 fields (7 from protocol 5 and 2 from protocol 6), and two patients treated with 2 fields (protocol 4b). When all the patients' whole-brain average doses are plotted against their peak brain doses, Figure 28 is generated. This figure shows that the risk of somnolence greatly increases above a whole-brain average dose of about 6 Gy-Eq. Figure 29 shows the actual dose response curve for this data. From this curve, it can be observed that at 6.1 Gy-Eq, the risk of producing somnolence is about 50%.

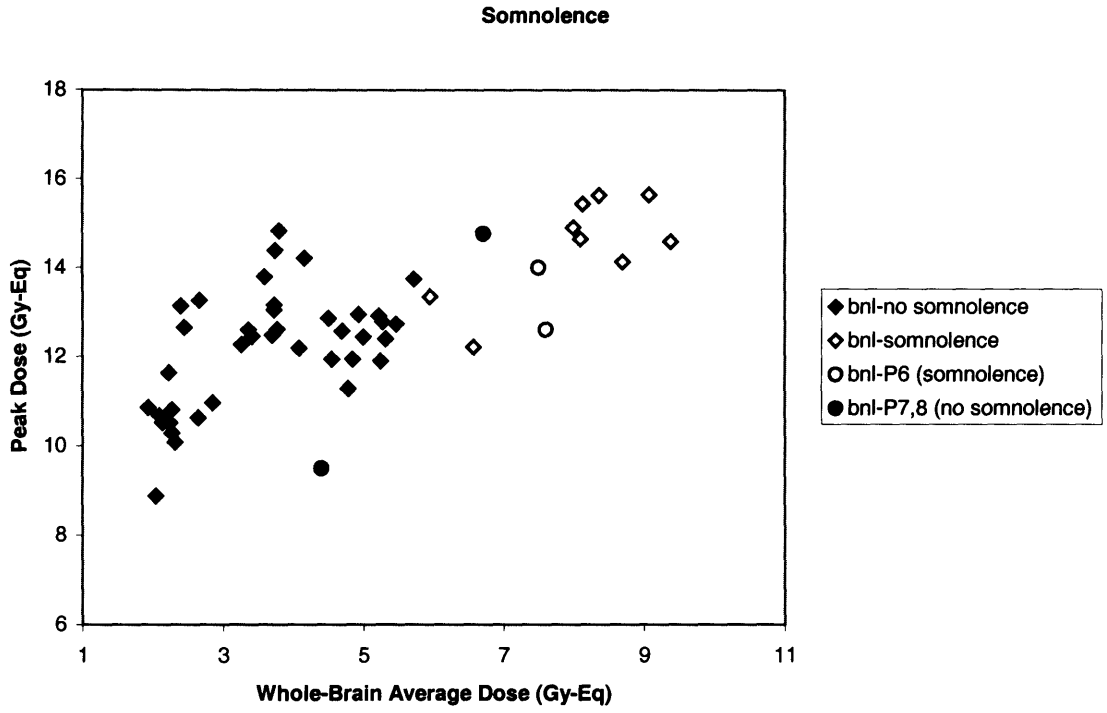

Figure 28: Original prescribed peak vs. whole-brain average weighted doses for all BNL patients with data on which patients showed somnolence following treatment

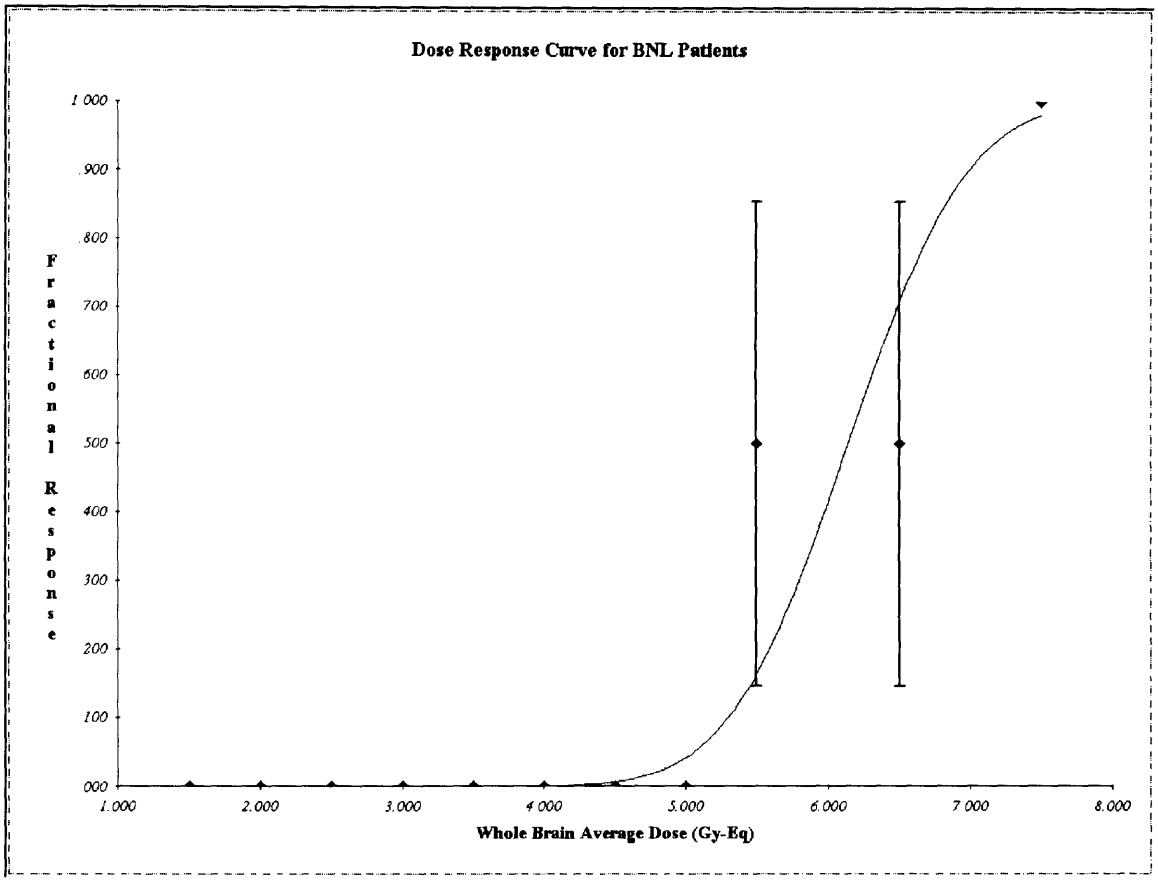

Figure 29: Dose response curve for somnolence for all BNL patients treated with BNCT

To get a more accurate representation of the cause of somnolence syndrome, the patients treated with the MIT M67 beam should be included in this study. With the BNL scaling factors determined previously based on the dosimetry intercomparison [9], this patient pooling can now be done. To do this, the BNL patient doses from Table 13 must now be used. When the BNL and M67 patient data are combined, Figure 30 is obtained. This figure shows MIT and BNL patients who did and did not exhibit somnolence, along with two MIT metastatic melanoma patients treated with BNCT, neither of which exhibited somnolence. This figure singles out the BNL patients in protocols 6, 7, and 8 because these patients were either treated with fractionated BNCT (protocols 6 and 7), or were treated for recurrent GBM (protocol 8), and therefore their treatment was different from the other BNL patients (protocols 1-5) and should be noted. From this figure, it is clear that there is no longer a clear-cut dose, either on the whole brain average axis or the peak dose axis, above which all patients exhibit somnolence and below which none

exhibit somnolence. It does appear, however, that patients receiving a whole-brain average dose of greater than about 5 Gy-Eq have a higher chance of exhibiting somnolence syndrome than those below this dose. By including patients from more clinical trials, a better idea of exactly what the relationship is between whole brain average dose and somnolence syndrome can be determined. Looking at a dose response curve, Figure 31 gives a better idea of the risk of causing somnolence associated with the various doses.

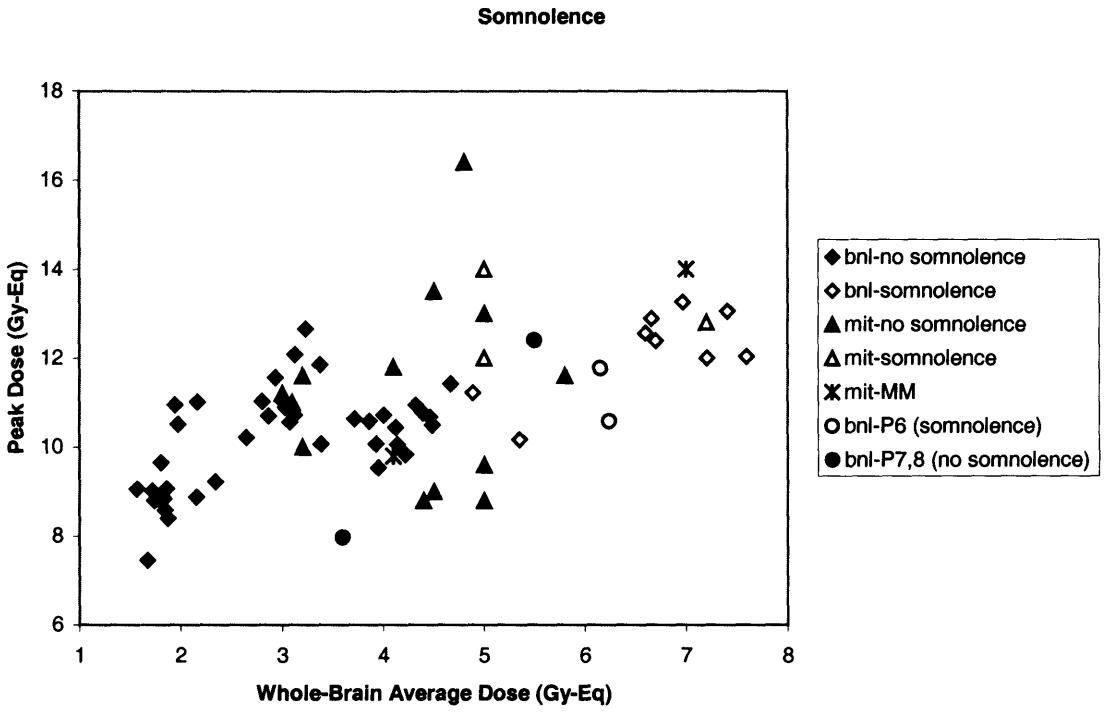

Figure 30: BNL and MIT patient peak vs. whole-brain average doses (adjustment factors applied to BNL patient doses) along with data on which patient showed symptoms of somnolence following treatment [1]

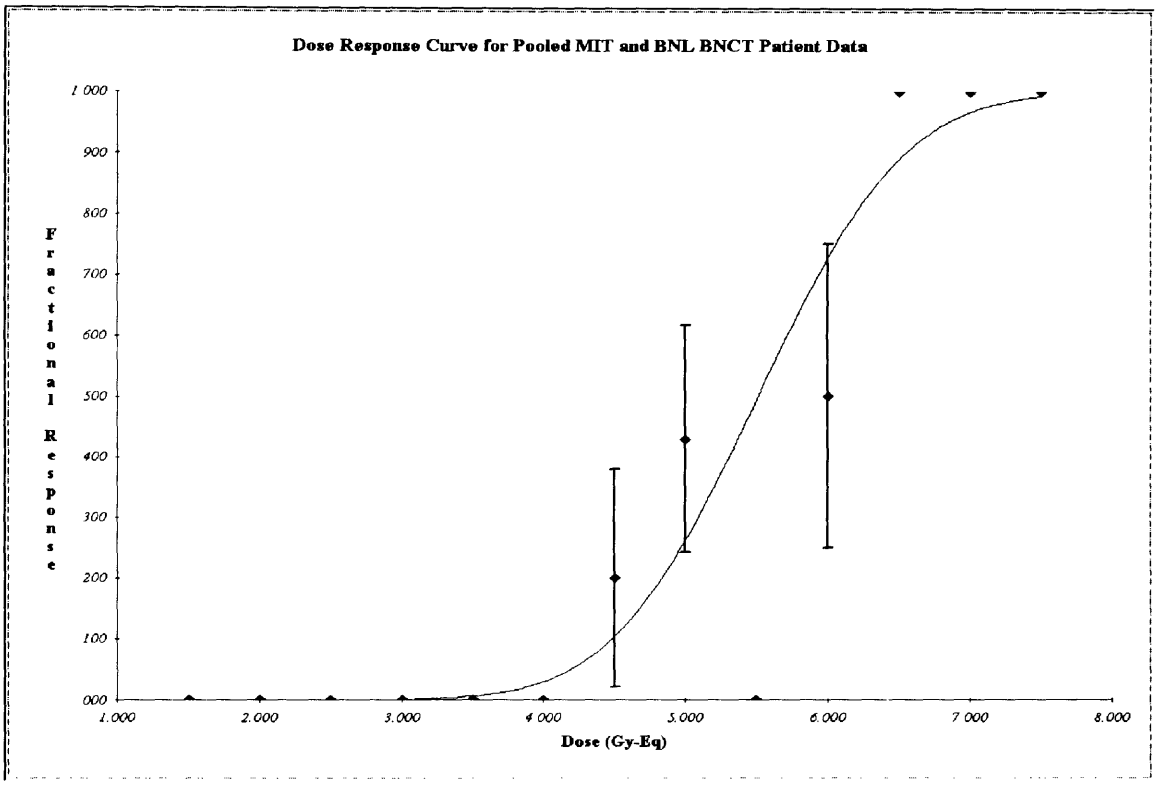

Figure 31: Whole brain average dose response curve for somnolence for pooled BNL and MIT patients

2. Patient Details

It is important to make sure that the patients included in the study do not have any abnormalities in their treatment or follow-up, and that there are no other factors that might influence whether or not the patient shows symptoms of somnolence. One major factor that must be taken into account in the pooling of patients is that different physicians are in charge of different patients. Because of this, and because somnolence is not a clear-cut endpoint, the physicians may not be scoring the somnolence in the same manner (i.e., while one physician might claim a patient is showing symptoms of somnolence, another might disagree). In calculating the dose response curve, it was decided that one of the MIT patients should excluded. This was the metastatic melanoma patient seen in Figure 30 to have a whole brain average dose of about 7 Gy-Eq. This patient was excluded from the dose responses curve because he or she received chemotherapy following the BNCT, and slipped into a coma before a full evaluation of whether or not he or she exhibited somnolence could be performed. Therefore, it is

difficult to say whether or not he or she showed symptoms of somnolence, and in fact after a discussion with the doctor monitoring the patient, it was decided that this patient might in fact have been exhibiting symptoms of somnolence, though it was never recorded. It is also important to remember that the BNL patients in protocols 6, 7, and 8 were either treated with fractionated BNCT or for recurrent GBM. Because this has no effect on the whole brain average dose received during the BNCT treatment, these four patients were left in the patient pool when calculating the dose response curve. All of the MIT patients also received fractionated BNCT (two fractions on consecutive days).

3. Dose response

It is important to look at a dose response curve for the patient data to determine a more precise correlation between absorbed dose and risk of somnolence. The whole-brain average dose-response curve of the BNL and MIT patients, after the adjustment factors have been applied to the BNL patients, can be seen in Figure 31. With the applied adjustment factors, the MIT and BNL patients can be combined, and with more patients in the pool of data, the numbers in the dose response curve will be more statistically significant. Ultimately, by combining patient data from all BNCT institutions, researchers will be able to determine with good accuracy the risk associated with administering various whole-brain average doses.

Figure 31 shows the dose response curve for the pooled patient data from BNL and MIT. In this figure, the x-axis shows whole-brain average weighted dose in Gy-Eq, and the y-axis shows the fractional probability of developing somnolence. From this plot, the whole-brain average dose required to produce 50% response in BNCT patients appears to be about 5.5 Gy-Eq. By administering a whole-brain average dose of just over 6.0 Gy-Eq, the treatment has a 75% chance of producing somnolence syndrome in the patient. From this patient data, it is impossible to determine what dose is required to produce 100% response, but it appears to be somewhere between 7 and 8 Gy-Eq. With additional patients included in the study, a more accurate dose response curve can be calculated.

References

1. P.M. Busse, O.K. Harling, M.R. Palmer, W.S. Kiger III, J. Kaplan, I. Kaplan, C.F. Chuang, J.T. Goorley, K.J. Riley, T.H. Newton, G.A. Santa Cruz, X-Q. Lu, R.G. Zamenhof, A critical examination of the results from the Harvard-MIT NCT program phase I clinical trial of neutron capture therapy for intracranial disease, Journal of Neuro-Oncology, **62:** 111-121 (2003).

2. A.Z. Diaz, Assessment of the results from the phase I/II boron neutron capture therapy trials at the Brookhaven National Laboratory from a clinician's point of view, J. Neuro-Oncol. **62:** 101-109 (2003).

3. P.J. Tofilon, J.R. Fike, The radioresponse of the central nervous system: a dynamic process, Radiat. Res., **153:** 357-370 (2000).

4. S. Faithfull, M. Brada, Somnolence syndrome in adults following cranial irradiation for primary brain tumors, Clinical Oncology, **10:** 250-254 (1998).

5. Y. Nakagawa, K. Pooh, T. Kageji, S. Uyama, A. Matsumura, H. Kumada, Clinical Review of the Japanese Experience With Boron Neutron Capture Therapy and a Proposed Strategy Using Epithermal Neutron Beams, Journal of Neuro-Oncology, **62:** 87-99 (2003).

6. J. Hopewell, Proposition: long-term changes in irradiated tissues are due principally to vascular damage in the tissues, Med Phys., **25:** 2265-2268, 1998.

7. J.C. Flickinger, D. Kondziolka, L.Dade Lunsford, A. Kassam, L.K. Phuong, R. Lisscak, B. Pollock, Development of a model to predict permanent symptomatic postradiosurgery injury for arteriovenous malformation patients, Int. J. Radiation Oncology Biol. Phys., **46:** 1143-1148 (2000).

8. J.C. Flickinger, D. Kondziolka, A.M. Kalend, A.H. Maitz, L.D. Lunsford, Radiosurgery-related imaging changes in surrounding brain: Multivariate analysis and model evaluation, Radiosurgery, **1:** 229-236 (1996).

9. K.J. Riley, P.J. Binns, D.D. Greenberg, O.K. Harling, A physical dosimetry intercomparison for BNCT, Med. Phys., **29:** 898-904 (2002).

VII. Conclusions and Future Work

1. Summary of Conclusions

This thesis makes it possible to pool BNCT patient data from two different clinical centers. This approach is desirable because of the small number of patients treated at any one center. By pooling patient data, it becomes easier to determine a cause of the somnolence endpoint and efficacy of BNCT as a function of dose.

In order to pool BNCT patient data, a number of differences between the BNCT centers had to be taken into consideration. The differences addressed in this thesis are tissue definition differences and dosimetry measurements. Once these differences were evaluated, the patient data were pooled, and a correlation between prescribed patient whole-brain average dose and the endpoint was determined. From this correlation, the tolerance of normal brain for somnolence was evaluated, which will be of great use in future BNCT trials.

While MIT uses a ^{14}N concentration of 2.2% in normal brain tissue, BNL used a ^{14}N concentration of 1.8% when calculating treatment plans for their respective BNCT patients. It was found that this difference leads to a difference in peak brain dose of less than 3%. Therefore, it was decided that this difference is small enough that no correction factor needed to be applied to the BNL patients because of the ^{14}N difference when attempting to pool patient data.

Systematic differences in dosimetry techniques were a major hurdle in the intercomparison process. By breaking down the beam components of the BNL beam, scaling factors between gamma, ^{14}N, ^{10}B, and fast neutron dose definitions in measurements between BNL and MIT were calculated. ^{14}N and ^{10}B dose measurements were found to be 8% lower when measured by MIT in the BNL beam, gamma dose measurements were found to be 26% lower, and fast neutron dose measurements were found to be 27% lower (when calculated from in-air measurements). This led to scaling factors of 0.92, 0.92, 0.74, and 0.73 for the ^{14}N, ^{10}B, gamma, and fast neutron doses, respectively. These scaling factors were applied to the BNL patient input files, which were then run through the RTPE treatment planning software, and adjusted peak and

whole-brain average doses were obtained for all patients treated at BNL. These new peak and whole-brain average doses were then used, in conjunction with the MIT patient peak and whole-brain average doses, to determine the correlation between the somnolence endpoint and dose. It was determined that there appears to be a correlation between whole-brain average dose and somnolence. When looking at the dose response curve for the combined MIT and BNL patient data, the probability of producing somnolence increases to 50% with a whole-brain average dose of about 5.5 Gy-Eq. This tolerance level is consistent with tissue tolerances previously published [1].

It is also important to note the error on these weighted whole-brain average dose values. The error on the MIT and BNL measurements were previously calculated, and, for the weighted dose values, range between about 5% and 15%, depending on the depth in tissue.

2. Recommendations for Future Work

While this thesis evaluated the differences between two BNCT facility's beams and normal tissue definition, this research is just the first step to a complete pooling of BNCT patient data. In order for it to be complete, a few other differences need to be examined and evaluated. The most predominant difference is the use of different treatment planning software systems. Differences in treatment planning systems arise mainly from methods used to calculate dose, but also occur due to differences in the way the patient geometry is modeled. Therefore, the next step in this process should be a complete evaluation of treatment-planning software programs.

In order to compare treatment-planning software, it is important to have a common phantom that can be or has been modeled and simulated using all the software programs. For instance, the MIT ellipsoidal water-filled phantom has already been run in NCTPlan. Additionally, access is available to CT scans of the head phantom, and it can thus be run through RTPE and the output can be compared to that of NCTPlan. Also, if access is available to MRI scans from a sample patient treated at MIT, this patient can be run in RTPE, and the treatment plan generated from this program can be compared against that generated from NCTPlan. In order to compare the treatment planning systems, the

results from this thesis must be taken into consideration, in order to eliminate the differences between different facility's measurements. Dosimetry intercomparisons have already been performed on the clinical epithermal neutron beams at 6 or 7 different centers [K. Riley, P. Binns, unpublished data].

It is quite important to note that different clinicians were in charge of the follow-up monitoring of the different BNCT patients, and different clinicians do not evaluate the somnolence endpoint in the same manner. This presents a significant source of error in the evaluation of a threshold for somnolence. In the future, it would be best to have a way for all clinicians to evaluate somnolence to eliminate this error.

Lastly, it will be important to apply a comparison such as the one outlined in this thesis to other BNCT clinical centers, specifically those using BPA-F. Including treatment centers that use BSH will necessitate other differences to be taken into consideration. The more patients that can be combined into one patient pool, the more accurate results can be obtained. For instance, a more accurate somnolence tolerance dose could be obtained by including the patients from the other BNCT clinical trials around the world. By understanding the systematic dosimetry differences between the BNCT clinical trials, this patient pooling can be done.

References

1. B. Emami, J. Lyman, A. Brown, L. Coia, M. Goitein, J.E. Munzenrider, B. Shank, L.J. Solin, M. Wesson, Tolerance of normal tissue to therapeutic irradiation, Int. J. Radiation Oncology Biol. Phys., **21:** 109-122 (1991).